

THESIS
C3328
1972
C.2

GEOLOGY OF PRECAMBERIAN
ROCKS OF THE EL ORO MOUNTAINS AND VICINITY
MORA COUNTY, NEW MEXICO

By

Joseph Charubini Cepeda

Martin Spence Memorial Library
New Mexico Institute of Mining & Technology
Cannon Station
Socorro, New Mexico 87801

Submitted to the Faculty of the
New Mexico Institute of Mining and Technology
in partial fulfillment of the requirements for
the degree of Master of Science in Geology

December 1972

ABSTRACT

The El Oro Mountains are located on the southeast flank of the Sangre de Cristo Range of northern New Mexico. Precambrian rocks are covered to the east and west by Paleozoic limestones and arkoses. The El Oro Mountains consist of antiformal structures with gneiss and migmatitic gneiss in the core, mantled by muscovite schist, banded gneiss, and amphibolites. The entire sequence is intruded by granitic pegmatite dikes up to 300 feet thick and several thousands of feet long.

There have been at least two periods of Precambrian deformation. The earlier deformation produced isoclinal, recumbent folding trending south-southwest, with a shear zone having the same trend. Subsequently, elongate domes with axes trending northeast-southwest, were formed. These structures have vertical eastern limbs and moderately dipping western limbs. This second deformation reoriented the earlier fold axes to south and southwest trends.

Amphibolite facies metamorphism accompanied both periods of deformation, approximating conditions of the upper almandine amphibolite facies.

The entire sequence, with the exception of the amphibolites and pegmatites, is interpreted as metasedimentary, as evidenced by the inhomogeneity and composition of the rock units. The amphibolites represent metamorphosed basic sills.

Faulting during the Laramide orogeny thrust the Precambrian rocks toward the east, where they rest against Paleozoic sediments.

TABLE OF CONTENTS

ABSTRACT.....	page 1
TABLE OF CONTENTS	page 1
LIST OF ILLUSTRATIONS	page 2
INTRODUCTION	page 5
Location	page 5
Geography	page 5
Purpose of Investigation	page 6
Method of Investigation	page 7
Acknowledgements	page 8
PRECAMBRIAN ROCK UNITS	page 9
Introduction	page 9
Granitic Gneiss	page 10
Muscovite Schist	page 15
Banded Gneiss	page 19
Amphibolites	page 22
Pegmatite Dikes	page 27
METAMORPHISM	page 34
PALEOZOIC ROCKS	page 37
STRUCTURAL GEOLOGY	page 38
Introduction	page 38
Folding	page 38
Faulting	page 53
Jointing	page 57
GEOLOGIC HISTORY	page 58
REFERENCES CITED	page 61

LIST OF ILLUSTRATIONS

Figure	Page
1A Quartzo-feldspathic banding within the gneiss	13
1B Pegmatite dike intruded into granitic gneiss	13
2A Feldspar aggregates in the amphibolite north of Cebolla Pass	23
2B Feldspar veins within the amphibolite	23
3A Feldspar crystal at boundary of pegmatite dike	28
3B Selvedge zone at boundary of pegmatite dike	28
4A Pegmatite dike	30
4B Pinch-and-swail structure of pegmatite dikes, as exhibited in roadcut east of Mora	30
5 Pressure and temperature conditions of metamorphism in the El Oro Mountains	35
6 Equal area projection of foliation poles in domain 1 ...	41
7 Equal area projection of mesoscopic fold axes in domain 1	42
8 Equal area projection of foliation poles in domain 2	43
9 Equal area projection of mesoscopic fold axes in domain 2	44
10 Equal area projection of foliation poles in domain 3	45
11 Equal area projection of mesoscopic fold axes in domain 3	46

Figure	Page
12 Diagram depicting method of determining attitude of B1 axes, by intersecting small circles, in stereographic projection	47
13A Asymmetric similar fold in Muscovite-rich gneiss	51
13B Chevron fold delineated by quartz-feldspar bands	51
14A Symmetrical chevron fold in granitic gneiss	52
14B Asymmetrical similar folding of quartz-feldspar band in biotite gneiss	52
14C Open mesoscopic fold in muscovite gneiss	52
14D Similar, asymmetrical folding of magnetite layers in gneiss ..	52
14E Similar, isoclinal mesoscopic fold, showing evidence of superposed folding in harmonic undulations of limbs	52
14F Similar folding with shear zone, parallel to axial plane of mesoscopic fold, delineated by quartzo-feldspathic material	52
15 Schematic diagram showing origin of Precambrian shear zone and adjacent amphibolites	54
16A Closely spaced, parallel jointing in granitic gneiss	55
16B Jointing in massive amphibolite	55
17 Equal area projection of poles to joints in Precambrian rock units	56
18 Sequence of events during the Precambrian in the El Oro Mountains	59

PLATES

Plate 1 Geologic Map of the El Oro Mountains and Vicinity In Pocket

Plate 2 Structure Contour Map In Pocket

TABLES

Table	Page
1 Modal composition of metamorphic rock units	12
2 Comparison of K-ray peaks for sillimanite from the El Oro Mountains, New Mexico, and Delaware County, Penn. ...	17
3 Modal composition of pegmatites	31
4 Summary of structural data plotted in stereographic projection	48

INTRODUCTION

Location

The El Oro Mountains are located in Mora County in north-central New Mexico. They form part of a south trending belt of Precambrian outcrops on the eastern slopes of the Sangre de Cristo Mountains.

The Sangre de Cristo Range is bounded by the Rio Grande Basin on the west, and the high plains of eastern New Mexico to the east.

The main population center in the map area is the village of Mora, located at the intersection of New Mexico Highways 3 and 94. It is 28 miles northwest of Las Vegas, New Mexico, and 65 miles southeast of Taos. Mora has a population of about 1500, and is the center of activities for a large rural population. Stanley [1963], states the following about the origin of the town:

"Originally named Santa Gertrudes de Mora, the present community was settled by 26 Mexican families to whom the Mora Land Grant was given in 1835 by Governor Albino Perez. The name Mora was probably chosen because of the great number of mulberry trees growing in the valley."

Other communities in the area include North Carmen and Ledoux.

During the dry season, the map area is readily accessible by state and county roads. During the wet months, July through September, the dirt roads in the area become impassable after several days of heavy rains.

Geography

Elevations in the map area range from 7140 feet at the southeastern

border of the map, to 8461 feet at Eagle Peak, in the center of the map area.

The region underlain by Precambrian gneiss is characterized by sharp peaks and ridges, and deep narrow canyons. The areas underlain by Precambrian amphibolite and schist, or Paleozoic rocks, consist of rounded hills. In areas where gneiss is the predominant rock type, the Precambrian-Paleozoic contact is characterized by a change from the dip-slope topography of the Paleozoic beds to the rugged, steep topography of the Precambrian terrane.

The north facing slopes, regardless of underlying rock type, are more densely vegetated than the opposite slopes; this is probably due to unequal amounts of solar radiation. Evaporation is less on the north facing slopes, which have therefore developed denser vegetation and a soil cover.

Vegetation on the slopes consists of scrub oak and different varieties of grasses. Conifers common in the area include, juniper, pinyon and ponderosa pine, and Douglas fir on the higher peaks and ridges. Aspen and cottonwoods are found in stream and canyon bottoms. The alluvium filled valleys exhibit a variety of grasses and shrubs.

Farming, ranching, and tourism are the main sources of income for the residents in and around Mora.

The alluviated valleys, including the Mora and Cebolla valleys, are planted with corn, oats, and alfalfa, at the start of the summer rainy season. The yield is used mainly as feed for cattle, which graze in the valleys.

Goats and sheep range through the more rugged portions of the map area.

Purpose of Investigation

The El Oro Mountains were selected for an investigation of the Precambrian geology with two primary goals;

1] To extend the mapping of Precambrian rocks in the Sangre de Cristo Mountains. The area immediately to the north had been mapped previously by Riese [1969], as a Master's thesis at New Mexico Institute of Mining and Technology.

2] To acquire a better understanding of the geologic, structural, and petrologic relationships in the Precambrian of the Sangre de Cristo Range.

The El Oro Mountains provide good outcrops, and a variety of different lithologic units whose field relationships are well exposed; moreover the area is easily accessible.

Method of Investigation

Geologic mapping at a scale of 1:24,000 on the United States Geological Survey 7 1/2 minute Mora Quadrangle, and collection of field data and samples was done during the summer of 1972. A total period of 2 1/2 months were spent in the field.

Specimens collected numbered more than 150, of which 60 thin sections were cut; ten of these were stained for detection of potassium feldspar.

Point counts [1000 points or more per section] were made on thin sections that were considered to be representative of the units described.

Aerial photographs provided by the New Mexico State Bureau of Mines and Mineral Resources were used to locate outcrops of Precambrian rocks, and to delineate contacts with the overlying Paleozoic sediments.

Acknowledgements

The author wishes to acknowledge financial support provided by the New Mexico Geological Society.

I also wish to express my sincere appreciation to Professor A. J. Budding who suggested the project, and without whose valuable assistance, criticism, and guidance this project could not have been completed. Appreciation is expressed to Professors Gale Billings and Kent Condie for their assistance and suggestions, and to Drs. Frank Kottlowski and C. A. Walker of the New Mexico State Bureau of Mines and Mineral Resources for their special assistance.

I am especially grateful to Mr. Lucas Valdez of Mora, for use of his ranch as a campsite; and to Mr. Tony Aragon of Ledoux for his special assistance.

PRECAMBRIAN ROCK UNITS

Introduction

The most abundant Precambrian rock type in the El Oro Mountains and vicinity is a granitic to migmatitic mica gneiss which forms the core of a broad anticlinal structure. The mica in the gneiss is either muscovite or biotite, while some gneisses carry both muscovite and biotite. Other major mineral constituents are quartz, microcline, and oligoclase in varying amounts.

The gneissic core of the anticlines is mantled by sillimanite-bearing muscovite schist, elongate amphibolite bodies, and a zone of banded gneiss which occurs northwest of the gneiss dome.

The schist and amphibolites are intruded by large, up to 300 feet thick, pegmatite dikes which parallel the foliation. Pegmatite dikes are also present in the gneiss, but they are of smaller size than in the schist or amphibolite.

The contacts between rock units, except for the pegmatites, are gradational and the lithologies interfinger with one another, over a distance of several feet.

Structural evidence shows that at least two periods of deformation have taken place during the Precambrian. Evidence of the earlier deformation is preserved as mesoscopic folds with an original south-southwest trend. Later deformation has reoriented these folds into south and southwest directions.

With the exception of the pegmatites and amphibolites, the units are extensively weathered, and collection of fresh samples is difficult.

Granitic Gneiss.

The granitic gneiss is a tan to buff, medium to coarse-grained rock. Where mica is abundantly present, it imparts a well-defined foliation to the gneiss. The foliation is locally enhanced by thin, concordant quartzo-feldspathic veins. In some cases this banding is so pronounced and pervasive that the rock becomes a migmatitic or veined gneiss. Quartz, microcline, muscovite, and plagioclase feldspar are the major constituents.

The gneiss is of two types; a biotite gneiss, and a muscovite gneiss. The latter is more abundant with foliation defined by muscovite flakes up to 1.5 millimeters long. The composition of the gneiss varies widely. Modal analyses were determined using a Swift point counter; 1000 to 1200 points were counted for each thin-section. See table 1. Changes in modal composition are gradational within the gneiss.

Well-defined, concordant quartzite beds, up to ten feet thick occur within the gneiss. Modal analysis of a thin-section of this quartzite is shown in table 1, as sample 727-49. Magnetite-rich layers within these quartzite beds, parallel the foliation. Magnetite banding represents original iron-rich layers in the sedimentary sequence; thus the magnetite banding defines original bedding, and foliation and original sedimentary bedding coincide.

In both muscovite and biotite gneiss, the quartz shows evidence of strain. Boundaries between adjacent quartz grains are sutured and undulatory extinction is present in all quartz grains. The xenoblastic grains are some of the largest in the gneiss, with diameters up to 4 millimeters.

Muscovite-quartz boundaries are concave to the muscovite, suggesting that muscovite has formed at the expense of the quartz.

Microcline crystals average about 1 millimeter in size, although some grains exceed 2 millimeters. Twinning, according to the albite and pericline laws, produces gridiron structure in the microcline. Some of the crystals are poikiloblastic, enclosing small, xenoblastic, quartz grains.

The thin-sections were stained with sodium cobaltinitrite [Bailey and Stevens, 1960] in order to distinguish potassium feldspar from plagioclase and quartz.

Plagioclase feldspar is represented by granoblastic, sericitized grains averaging about 0.5 millimeter in size. The anorthite component of the plagioclase feldspar was determined by the Michel-Levy method, and averages 26 per cent.

Foliation in the gneiss is expressed by muscovite laths up to two millimeters by 0.2 millimeters. The elongate grains are strongly oriented parallel to each other, defining the foliation. Smaller, equidimensional grains are less strongly oriented. In general, microcline-muscovite boundaries are concave to the microcline.

The average composition of the more abundant muscovite gneiss is; quartz 40.2%, potassium feldspar 27.5%, plagioclase feldspar 18.7%, and muscovite 8.7%.

Biorite is present as small, stubby, granoblastic grains. Average grain size is about 0.8 millimeters by 0.2 millimeters, although some crystals exceed two millimeters in the longest dimension. The pleochroic formula is X= yellowish brown, Y= reddish brown, Z= dark brown.

Table 1.

Modal Composition [in volume per cent]
of Metamorphic Rock Units

Sample No.	Rock Unit	Quartz	Potassium Feldspar	Plagioclase Feldspar	An Content	Muscovite	Biotite	Magnetite	Hornblende	Hematite	Calcite	Epidote
727-39	Gneiss	43.2	23.6	15.4	23	17.0		1.3		tr		
727-3	Gneiss	36.3	42.2	16.8	33	0.3		1.2		1.9		
727-6	Biotite Gneiss	27.0	28.7	28.2	24		4.3	0.8		11.4		
727-29	Biotite Gneiss	31.4	27.3	27.5	25		10.0	1.4		2.1		
727-12	Gneiss	40.6	19.6	17.3	36	19.5		3.0		tr		
727-10	Gneiss	68.1	6.1	5.6	30	21.0						
727-7	Gneiss	48.2	30.5	8.1	29	12.6		0.9		tr		
727-19	Biotite Gneiss	42.5	30.5	22.5	24		5.0	0.3		tr		
727-25	Gneiss	24.3	39.5	26.9	20	7.8		0.6		1.0		
727-49	Quartzite	73.9				2.5		23.6				
727-51	Musc. Schist	36.5	0.1	21.1	15	33.8	4.1	3.1		tr		
727-52	Musc. Schist	38.8	0.2	0.3	14	47.2	9.4	4.6				
727-53	Banded Gneiss	46.6	1.5	10.5	26	39.0	0.5	0.1		0.9		
727-54	Banded Gneiss	56.2	11.5	12.5	28	18.8		1.1		0.3		
727-55	Banded Gneiss	58.7	16.0	13.4	28	10.5		1.8				
727-2	Amphibolite	5.7		34.0	48			0.5	59.8			
727-13	Amphibolite	1.6		51.8	58			4.4	41.6			
727-9	Amphibolite	3.5		33.9	60			2.4	59.2		0.3	0.1
727-30	Amphibolite	0.5		44.0	48				55.7			

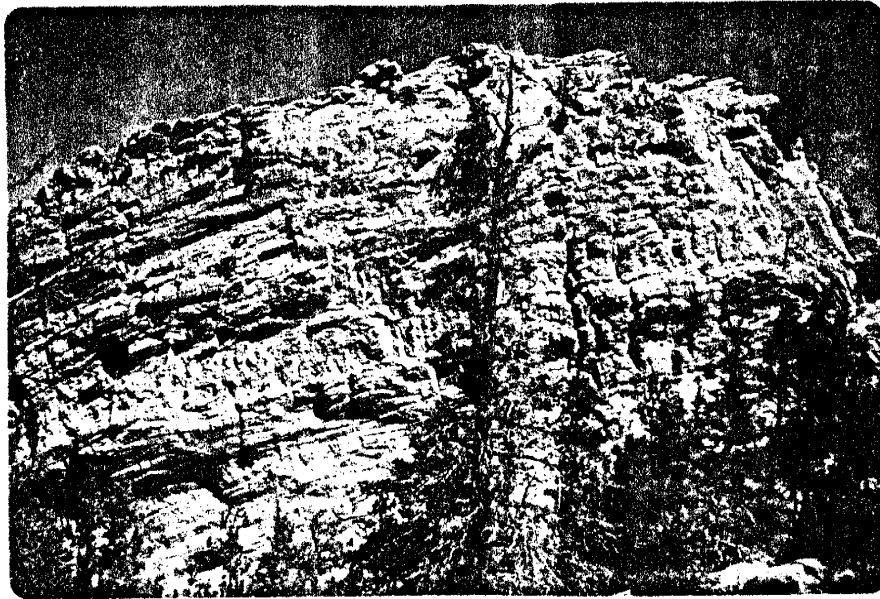
Figure 1.

- A Quartzo-feldspathic bands parallel to foliation within the gneiss. Photograph taken northwest of Eagle Peak

- B Pegmatite dike in gneiss. Photograph taken from point north of Eagle Peak, looking north.



A



B

LIBRARY
N. M. I. C. T.
SOCORRO, N. M.

In some samples, the biotite grains are dimensionally unoriented, suggesting that at least some of the biotite formed or recrystallized subsequent to the deformational phase responsible for the development of foliation.

Two minerals commonly occur as small, granoblastic to idioblastic grains in the gneiss. In the area north of Eagle Peak, reddish-brown idioblastic crystals of garnet are found in the gneiss. In the south-central part of the map area, just north and west of the El Oro Mountains, xenoblastic magnetite grains up to 0.5 millimeters in diameter are disseminated throughout the gneiss. The magnetite content is sufficient to deflect the compass needle by over forty degrees, when the compass is placed against the outcrop. In some samples, magnetite-rich bands, similar to those in the quartzite beds, occur. Near by, pegmatite dikes are also very rich in magnetite, with magnetite nodules several inches in diameter.

The enrichment of magnetite in the pegmatites, in areas where there is a similar abundance of magnetite in the gneiss, suggests that the pegmatites may have been derived, at least in part, from the gneiss.

The inhomogeneity of the gneiss suggests that it is of metasedimentary origin. The original rock was probably a quartzo-feldspathic sandstone, with interbedded, iron-rich, quartz-arenite beds. The low variation in anorthite component in the plagioclase suggests that the sandstone was a weathering product of an older igneous rock, probably a granite.

Muscovite Schist

Muscovite schist, which mantles the gneiss, contains muscovite and quartz, with lesser amounts of feldspar and sillimanite. Garnet, epidote, zircon, biotite, and magnetite are present in small or trace amounts.

Muscovite crystals reach sizes up to 5 millimeters by 0.2 millimeters, oriented parallel to each other, producing a well-defined foliation. Small grains of sillimanitized quartz are disseminated throughout the schist in trace amounts. Muscovite makes up about 40 per cent of the rock.

Xenoblastic quartz grains are present in two size ranges. Equidimensional grains average less than 0.5 millimeters in diameter. Larger, elongate crystals oriented with the long axis parallel to the foliation, reach sizes up to one millimeter in the long dimension. Quartz has concave boundaries with the feldspar, and makes up 37.5 per cent of the muscovite schist.

The strongly sericitized plagioclase feldspar has a grain size slightly smaller than the larger quartz grains; the elongate grains of feldspar also parallel the foliation. Anorthite content of the plagioclase is An 15. Plagioclase feldspar constitutes 12 per cent of the rock.

Potassium feldspar occurs in small amounts, as small xenoblastic grains.

Magnetite is disseminated throughout, as polygonal grains 0.05 to 0.2 millimeters in diameter.

Epidote, distinguished by its yellowish-green color, forms elongate, xenoblastic grains up to three millimeters long. It occurs within muscovite crystals, where it has spread the cleavage planes apart.

Red-brown garnets are abundant in the schist adjacent to pegmatites, but are present throughout in trace amounts.

Blue-black sillimanite nodules up to three inches in diameter weather out of the schist at two localities; south of Eagle Peak, where a small lens of muscovite schist is found within the gneiss, and, east of the village of Mora and south of New Mexico Highway 3. The nodules are lens-shaped and lie with their smallest dimension perpendicular to the foliation of the schist.

In thin-section, the nodules appear as a mass of compacted, felty, microfolded fibers of sillimanite. Small [0.1 to 0.2 millimeter] grains of quartz are scattered within the aggregate. The nodules contain approximately 95 per cent sillimanite and 5 per cent quartz.

X-ray diffraction analysis on a nodule collected south of Eagle Peak, confirmed the presence of sillimanite and the very low quartz content, as evidenced by the weak quartz peaks. A listing of the sillimanite peaks from this sample is shown in Table 2.

The schist is approximately 500 feet thick, although it thins to the south and is not present as a mappable unit near the southern edge of the map area.

The unit is gradational with the gneiss, and lenses and stringers of muscovite schist are present in the gneiss in areas well removed from the schist-gneiss contact. For example, at Eagle Peak the gneiss has a greater quartz and muscovite content than the average gneiss. Five hundred feet to the south, the muscovite content approaches that of the schist, with a concomitant decrease in feldspar. Sillimanite nodules are present in the rock at this point. Three hundred feet further south, the rock

Table 2.

Sillimanite from Delaware County, Pennsylvania			Sillimanite from El Oro Mountains, Mora County, New Mexico	
d- Spacing	2-theta for Cu K-alpha radiation	Relative Intensity	2-theta for Cu K-alpha radiation	Relative Intensity [visually estimated]
3.42	26°	100	25.9°	strong
2.90	30.8°	40		
2.70	33.2°	40	33.4°	moderate
2.55	35.0°	70	35.3°	weak
2.42	37.0°	30	37.1°	weak
2.28	39.4°	40		
2.20	40.8°	80	40.9°	weak
2.12	42.6°	40		
1.98	45.6°	20	45.5°	weak
1.87	48.6°	30	48.6°	weak
1.83	49.8°	30		
1.80	50.3°	20	51.1°	weak
1.71	53.6°	40	53.6°	moderate
1.69	54.2°	60	54.4°	weak
1.59	57.8°	30	57.6°	weak
1.56	59.2°	30		
1.52	60.8°	80	60.8°	weak

has the mineralogy and texture of the average gneiss.

The muscovite schist-amphibolite contact is marked by gradational changes within both units. In the vicinity of the contact, the muscovite schist contains hornblende while the massive amphibolite shows a foliation.

The lensic nature, and gradational compositional variation of the muscovite schist suggest that it has been derived from a sedimentary rock. In view of the high muscovite content, the original sediment may have been an aluminous shale.

Banded Gneiss

A fine-grained, gray to tan, banded gneiss outcrops in two places in the map area. An outcrop about 300 feet wide is exposed within the amphibolite west of the village of Ledoux. It is concordant with the foliation, and the contact with the amphibolite is sharp. Banding is expressed by alternating muscovite-rich and quartzo-feldspathic bands.

In the area northwest of Cebolla Pass, a similar fine-grained rock of about the same thickness is present in a small syncline. It occurs between the gneiss and amphibolite. Lenses of amphibolite are present within the banded gneiss, whose contacts with the granitic gneiss and amphibolite are gradational. In parts of this outcrop, the banding is very pronounced, while in other portions, banding is not present.

In the banded portions of the gneiss, the dark bands have larger contents of magnetite and muscovite, while the light bands are predominantly quartz and feldspar. The banding, where present, is parallel to the foliation and the amphibolite-banded gneiss contact.

The most striking feature of the unit is its small grain size. Grains of equidimensional feldspar and quartz do not exceed 0.4 millimeter in diameter, except for a few porphyroblastic poikiloblasts of muscovite and potassium feldspar. Porphyroblasts enclose grains of all the other minerals in the rock.

The term "banded gneiss" is used in this paper in a descriptive sense. Banded gneisses [Berthelsen, 1961] are made up of alternating, well-defined layers of different composition. The layers may be less than one centimeter thick in thinly banded gneisses.

According to Dietrich [1960], there are diverse possible origins for banded gneisses. The banding is only partly the result of metamorphic differentiation, rather the pre-metamorphic banding was accentuated by recrystallization. Several sedimentary, igneous, and tectonic processes may produce a banded gneiss.

Petrofabric observations may provide evidence for favoring one genesis over another [Dietrich, 1959], although in some cases recrystallization can mask all pre-existing fabric elements.

Any interpretation concerning the origin of the banded gneiss, should explain the following observations;

- 1] The banded gneiss is compositionally similar to the granitic gneiss. However, the granitic gneiss is not banded.
- 2] No igneous or sedimentary textures can be identified in the banded gneiss.
- 3] The unit occurs only in the northwest portion of the map area.

Published photographs of blastomylonites [Quensel, 1917] show a banded rock with differing widths and intervals between bands, very similar to the banded gneiss. It is suggested that the banded gneiss is a product of shearing and metamorphic differentiation. Intense shearing along a northeast-striking plane produced a fine-grained banded rock. Later, metamorphism accentuated the banding and obliterated all evidence of cataclastic textures. Shearing within this localized zone probably occurred during a reduction of pressure and temperature conditions between the two periods of metamorphism. The later episode of metamorphism erased all evidence of shearing

Mechanical differentiation by shearing and metamorphic recrystallization have been the main processes which transformed an arkosic sandstone into the banded gneiss. Subsequently, the banded gneiss was folded into a small syncline north of Cebolla Pass.

Amphibolites

The amphibolite is a dark green to black, medium to coarse-grained hornblende and plagioclase-bearing rock. The thickness of amphibolite varies, but on the average, it exceeds 1000 feet. Contacts with the muscovite schist are gradational, with the amphibolite acquiring a foliation at the boundary. Lenses of amphibolite up to 60 feet long intrude the banded gneiss at the contact. A concordant lens of amphibolite is also found in the granitic gneiss, east of Mora. In general, the contact with the granitic gneiss is sharp.

Quartz-plagioclase veins and stringers lie concordant with the foliation. See figure 2B.

The amphibolites are intruded by pegmatite dikes up to 200 feet thick, however, the dikes are not as large, nor as abundant as those within the muscovite schist.

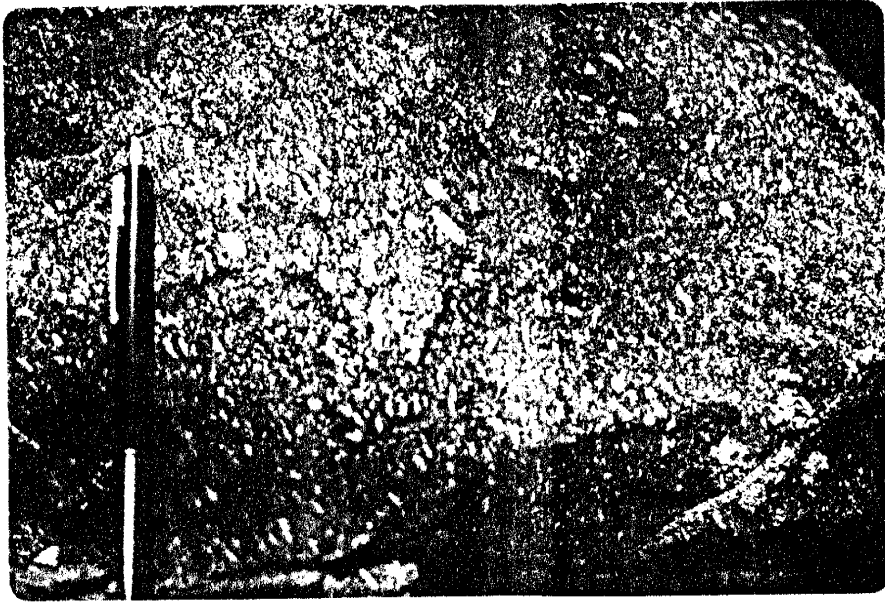
Amphibolites and muscovite schist are closely associated throughout the map area, except near the southern edge, where the muscovite schist is missing. Contacts were mapped on the basis of the most abundant lithology present.

Hornblende occurs as elongate, xenoblastic grains up to one millimeter long. Lens-shaped aggregates may contain almost 100 per cent hornblende as prisms up to 0.7 by 4 millimeters. Parallel orientation of these prisms define a mineral lineation parallel to the the mesoscopic fold axes in the area.

Two types of hornblende may be distinguished in the amphibolite, by their respective pleochroic colors. In the fine-grained, xenoblastic portions of the amphibolite, the hornblende is blue-green. The pleochroic

Figure 2.

- A Feldspar aggregates within the amphibolite north of Cebolla Pass; these are interpreted as relict phenocrysts.
- B Feldspar-rich stringers and veins within the amphibolite.
Photograph taken at roadcut east of Mora.



A



B

SOCORRO, N.M.

formula is, X= olive green, Y= yellowish green, Z= blue-green. This hornblende is usually xenoblastic, and occurs as stringers, aggregates, or clots.

In the region northwest of Cebolla Pass, many of the amphibolite samples have grains of granoblastic, yellowish brown hornblende. The amphibolites of this area also contain plagioclase crystal aggregates, figure 2A.

According to Shido and Miyashiro [1959], the hornblende changes from a blue-green variety, characteristic of the almandine-amphibolite facies, to greenish brown at higher metamorphic grades.

Studies in the Adirondack Mountains [Engel and Engel, 1962], have shown that amphibolite of the almandine-amphibolite facies contains blue-green hornblende, andesine, and quartz. The brown hornblende characteristic of higher metamorphic grades is richer in titanium and poorer in ferric iron than the blue-green hornblende of amphibolite facies rocks.

Lower ferric iron content is sufficient to change the color of the hornblende [Binns, 1965]. The brown hornblende has a granular texture as opposed to the ragged character of the blue-green hornblende.

It is interesting to note that the presence of brown hornblende has been recorded [Engel and Engel, 1962] in metagabbros.

The granular texture of the hornblende, the presence of plagioclase aggregates interpreted as relict plagioclase phenocrysts, and, the brown color of the hornblende, suggest that this hornblende is relict igneous hornblende. The original rock was probably a gabbro, or hornblende gabbro, intruded as sills, into the metamorphic sequence.

SOCORRO, N.M.

The hornblende content of the amphibolite ranges from 42 per cent to 60 per cent, with an average, of four thin-sections, of 54 per cent. See Table 1.

Plagioclase feldspar ranges from 34 per cent to 52 per cent of the amphibolite, by volume. The plagioclase grains are granoblastic, and most show good albite twinning. The anorthite content of the plagioclase ranges from An40 to An60. The grains are strongly sericitized along fractures and cleavage planes. They range from 0.2 to 0.5 millimeter in size.

A small amount of quartz is present as small, clear, xenoblastic grains, easily distinguished from the sericitized, cloudy feldspar. The grains average 2 to 3 millimeters in diameter. Some of the quartz is secondary, present primarily as vein fillings. The amphibolite contains 2.8 volume per cent quartz.

Magnetite is present in two size ranges within the amphibolite. Grains up to one millimeter, with square or rectangular cross-sections are disseminated throughout. Xenoblastic aggregates of magnetite up to two millimeters long are present around hornblende grains. Grains of both types look identical in reflected light.

Calcite is present in trace amounts in sample 727-9. It appears to be a secondary mineral wedged between hornblende crystals.

Rutile, ranging in size from 0.05 to 0.2 millimeters, is present in small amounts within xenoblasts of hornblende. It is possible that changes in hornblende composition caused by retrograde metamorphism, expelled titanium from the hornblende lattice, forming rutile.

Aggregates of plagioclase feldspar up to 2.5 by 7 millimeters occur northwest of Cebolla Pass. The grains in the aggregates have excellent

LIBRARY
 NATIONAL
 GEOGRAPHIC
 SOCIETY
 WASHINGTON, D. C.

albite twinning. The anorthite content, by the Michel-Levy method is An 40. Individual grains within the aggregates reach sizes up to one millimeter in the longest dimension. The feldspar aggregates are not found in the amphibolite in other parts of the map area, and, it is likely that these plagioclase crystals are of an igneous origin, and, that metamorphism has obliterated the igneous textures elsewhere.

The presence of relict phenocrysts, dikes of amphibolite within the schist, granitic gneiss, and banded gneiss, and, relict igneous brown hornblende, suggest that the amphibolites represent metamorphosed igneous rocks. Their lensic shape indicates they were probably intruded into the sequence as gabbroic sills. Some fine-grained amphibolites may represent metamorphosed basic flows.

5000000000
NORTH
WESTU.S. GEOLOGICAL SURVEY
WASHINGTON, D.C.

Pegmatite Dikes

Pegmatite dikes intrude all Precambrian units in the map area, but they are most abundant in the amphibolites and muscovite schist. They vary in thickness from a few inches to more than 300 feet, and individual bodies are lens-shaped. This pinch-and-swell structure of the pegmatites is very well illustrated in the roadcut east of Mora. See figure 4. Pinch-and-swell structures are indicative of a low pressure gradient, where a rock behaves in a ductile manner [Rivalenti and Sighinolfi, 1971].

Dikes, with very few exceptions, are concordant to the foliation, and discordant dikes are small and thin, and often folded or offset by small faults.

The pegmatites have a bimodal grain size distribution. Large crystals, 6 inches to 12 inches in length "float" in a groundmass whose grain size averages 2 to 4 millimeters.

In the fine-grained portion, microcline forms the largest crystals. It is present in sizes up to 4 millimeters in the longest dimension. It shows excellent twinning in two directions; some grains are poikilitic, enclosing small [0.1 to 0.2 millimeters] quartz and albite twinned plagioclase feldspar grains.

Anhydrous plagioclase grains range up to 3 millimeters in maximum diameter, with albite twin planes slightly bent or offset in some grains. This suggests the pegmatites were intruded during the last stages of the tectonic deformation. The anorthite content, by the Michel-Levy method, is An₁₀ to An₁₅.

Quartz is present as anhedral grains up to 3 millimeters in the longest

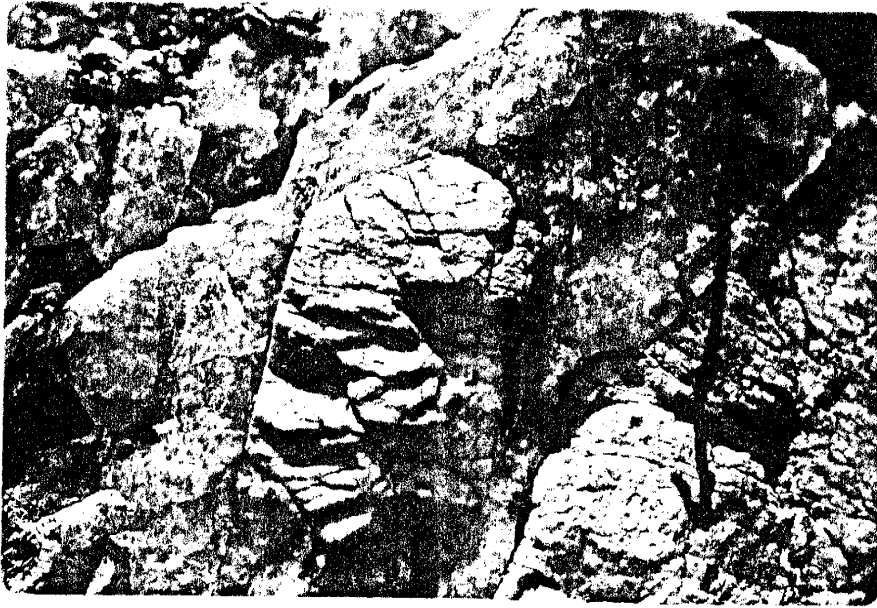
NATIONAL ARCHIVES
 SOOCHOW, N.M.

NATIONAL ARCHIVES
 SOOCHOW, N.M.

Figure 3.

A Feldspar crystal at boundary of pegmatite, at the mine south of Mora. Length of double-ended black line is four inches.

B Selvedge zone developed in pegmatite intruded into muscovite schist. Hammer is 14 inches long. Photograph taken at mine south of Mora.



A



B

dimension. In places, it has overgrown and enveloped adjacent microcline grains, giving the quartz a poikilitic texture.

Muscovite occurs as small, equidimensional grains up to one millimeter in diameter. Muscovite grain boundaries are concave to the quartz and convex to the microcline. Point counts [1000 points per thin-section] on two thin-sections of the fine-grained portion indicate that it has a granitic composition, with a large variation in relative amounts of feldspar, quartz and muscovite. However, the anorthite content of the plagioclase feldspar is approximately An12, in both samples.

The coarse-grained portion of the pegmatites consists of blocks of muscovite, quartz, plagioclase feldspar, and microcline-quartz intergrowths. Large crystals, up to 8 inches in the longest dimension, "float" in the fine-grained matrix described above.

A macromodal analysis of three pegmatites, numbered P1, P2, and P3 from north to south in the map area, was made in the field, using a six inch spacing along the line of traverse and a twelve inch spacing between traverse lines. Traverses were made perpendicular to strike, using a 22 ft. string marked at six inch intervals. The results are listed in Table 3.

Textural and mineralogical zoning is present in and adjacent to the pegmatites. In general, grain size increases toward the center of the pegmatite dikes. Mineralogical zoning, with quartz, plagioclase, and muscovite along the borders and microcline towards the center, is evident in some pegmatite dikes ranging in thickness from a few inches to over 50 feet. This potassium feldspar-rich central zone represents the last liquid in a pegmatite crystallizing from the edges toward the center [Cerny, 1971]

LIBRARY
MAR 11 1971
SODORHO, N.M.

U.S. GEOLOGICAL SURVEY
LIBRARY

Figure 4.

A Pegmatite dike, 40 feet thick, intruded into schist east of the village of Mora.

B Pegmatite dike intruded into amphibolite, showing pinch-and-swell structure, in roadcut east of Mora.



A



B

U.S. GEOLOGICAL SURVEY
WASHINGTON, D. C.

PHOTOGRAPHY
SECTION
WASHINGTON, D. C.

Table 3.

Modal Composition of Pegmatites [in volume per cent]

Sample No.	Rock Unit Intruded	Quartz	Muscovite	Plagioclase Feldspar	Microcline
P1	Muscovite Schist	29.8%	18.0%	49.4%	2.2%
P2	Muscovite Schist	23.3%	11.8%	62.0%	3.0%
P3	Muscovite Schist	26.0%	12.7%	47.2%	13.6%

Note: Percentages calculated from 500 points per pegmatite; P1 and P2 contain trace amounts of garnet and tourmaline.

AMERICAN
GEOLOGICAL
SURVEY
WASHINGTON, D.C.

Almandine, black tourmaline, and muscovite are present at wallrock-pegmatite boundaries, increasing in abundance with proximity to the boundary and size of the pegmatite. Selvedge zones are present at the boundaries of some pegmatites intruded into the muscovite schist.

One possible source of the pegmatites is the granitic gneiss. A partial melting of the gneiss, which has taken place, as evidenced by the migmatitic character of the gneiss in the El Oro Mountains, could yield a melt of the composition of the pegmatites. This source is further suggested by the presence of magnetite nodules up to several inches in diameter, within the pegmatites in the southern part of the map area. The pegmatites do not contain more than trace amounts of magnetite anywhere else. It is only in this area that the gneiss and the quartzite beds within it, contain appreciable amounts of magnetite, and a similar enrichment in the pegmatites suggests that the pegmatites are genetically related to the gneiss.

Experimental work on the granite system [Luth and others, 1964] has delineated the composition of minimum melts from 500 bars to 10,000 bars water pressure. The composition of the pegmatites of the El Oro Mountains, as determined by modal analyses, correlates with the composition for a minimum melt at a water pressure of 4000 to 5000 bars. The temperature at the eutectic at this water pressure is approximately 650°C.

A large water content is plausible, due to the presence of muscovite. At a pressure of 5000 bars, muscovite would not crystallize at temperatures around 700°C unless the water content of the melt amounted to about 8 weight per cent [Jahns and Burnham, 1969].

Granite pegmatites vary in mineral composition with depth of production. According to Schmakin [1971], muscovite-bearing pegmatites are produced at a pressure of 5 to 8 kilobars.

The evidence presented, together with the experimental work cited, suggest that the pegmatites of the El Oro Mountains were formed at 4 to 6 kilobars water pressure and an accompanying temperature of about 650°C. These conditions are in agreement with the pressure-temperature conditions of metamorphism for an assemblage containing migmatitic gneiss and sillimanite.

The pressure-temperature regime of metamorphism is further discussed in the section on metamorphism.

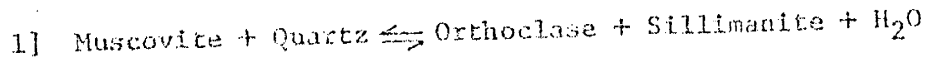
000000
N 1000
LIBRARY

METAMORPHISM

During regional metamorphism, the rocks in the El Oro Mountains were subjected to conditions of the upper amphibolite facies. The evidence for this statement is the following:

- 1] The presence of sillimanite, which is a characteristic mineral of the upper amphibolite facies, in the muscovite schist.
- 2] The migmatitic nature of the gneiss. At high water pressures partial melting of gneissas begins at a temperature of 650° to 700°C [Winkler, 1967].
- 3] The coexistence of muscovite and quartz, which places an upper limit on the pressure and temperature conditions of metamorphism.

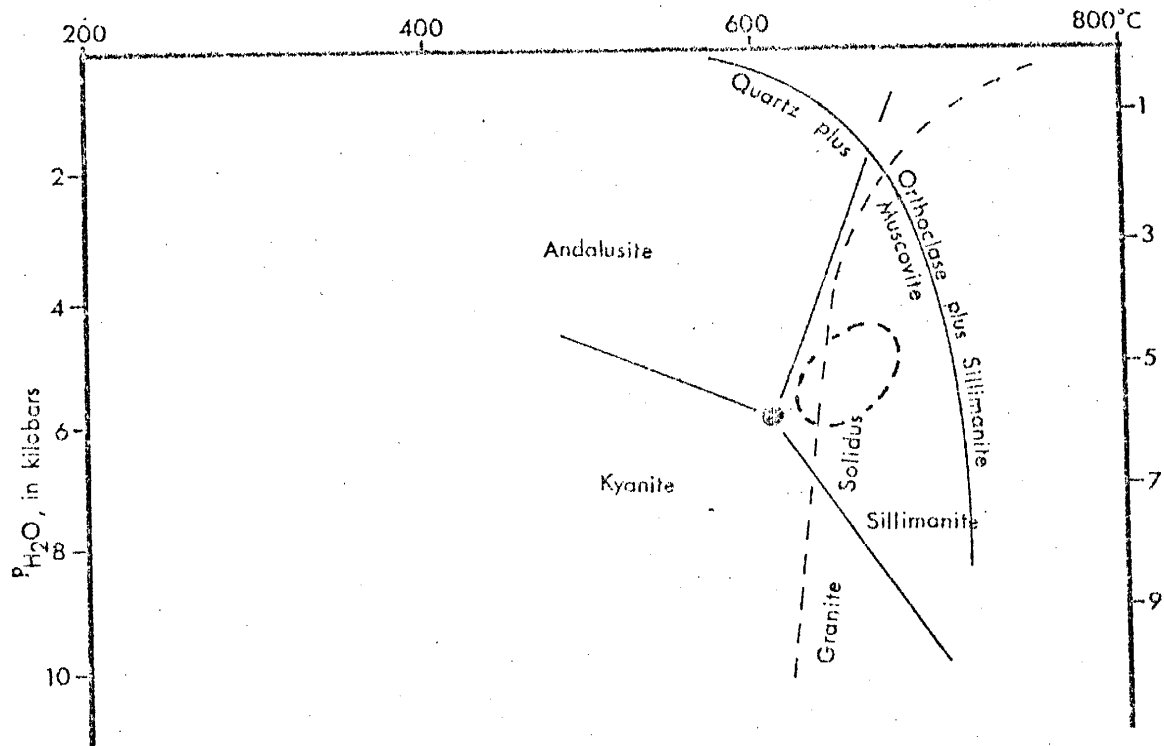
In the sillimanite-almandine-orthoclase subfacies of the amphibolite facies, the pertinent equation is,



In the El Oro Mountains, the pressure-temperature conditions necessary for this reaction to proceed to the right were not reached, because we do not find sillimanite in the absence of muscovite, in the metamorphic rocks. However, at pressures lower than those of the Barrovian facies series, sillimanite can coexist with muscovite [Winkler, 1967]. This sillimanite is not produced according to equation [1], but from kyanite or andalusite changing to sillimanite as the pressure-temperature conditions neared the stability field of sillimanite. The zone of coexistence of sillimanite and muscovite is called the first sillimanite zone by Winkler [1967].

Figure 5.

Pressure and temperature conditions of metamorphism



Probable pressure-temperature region for metamorphism in the El Oro Mountains

Aluminum silicate triple-point from Richardson and others [1969], granite solidus from Luth and others [1964], and muscovite plus quartz stability boundary from Evans [1965], and Segnit and Kennedy [1967].

Examination of ACF diagrams indicate that the muscovite schist has a composition appropriate for the formation of cordierite in the upper amphibolite facies of the Abukuma facies series. The absence of cordierite suggests that the pressure reached during regional metamorphism, was intermediate between the Barrovian and Abukuma facies series.

From the considerations discussed, a range of probable pressure-temperature conditions of metamorphism, can be delineated. The range of pressure and temperature values of the aluminum silicate triple point will not greatly affect the conclusions drawn regarding the pressure and temperature of metamorphism. The highest temperature of metamorphism was in the vicinity of 650° to 700° C, with an accompanying pressure of 4 to 6 kilobars.

The mineralogy of the pegmatite dikes, as discussed earlier, is in agreement with these P-T conditions.

These conditions prevailed beyond the latest stage of folding, as there is no evidence for large scale cataclastic textures or retrogressive metamorphism, in the metamorphic rocks.

37
PALEOZOIC ROCKS

Paleozoic rocks overlie the Precambrian unconformably on Amola Ridge to the east, and in the higher portions of the Sangre de Cristo Mountains to the west. The Precambrian-Paleozoic contact has a relief of several tens of feet, in the northwest part of the map area.

The sedimentary unit immediately overlying the Precambrian is a tan to gray limestone on the order of 50 to 100 feet thick. Above this unit is the Sandia formation of Pennsylvanian age, a coarse-grained arkose with abundant crinoid fragments.

Laramide deformation has thrust the Precambrian to the east, against the Paleozoic sediments. Mapping of faulting within the Paleozoic was not attempted. There is a prominent reverse fault, or faults, whose trace approximates the eastern edge of Precambrian outcrops, from a point east of the village of Mora, to the southern edge of the map.

In areas not adjacent to Precambrian outcrops, Paleozoic rocks were differentiated from alluvium by mapping on aerial photographs.

STRUCTURAL GEOLOGY

Introduction

The main structural feature of the El Oro Mountains are a number of domal or antiformal structures, as shown in plates 1 and 2. The core of the domes is, typically, a gneiss or migmatitic gneiss, granitic in composition, and mantled by other metasediments. Sheared and isoclinal folds are present in the gneiss and mantling units. Evidence for at least two distinct periods of deformation during the Precambrian, in the El Oro Mountains, will be presented.

Folding

The latest deformation has produced broad, doubly-plunging antiformal structures trending northeast-southwest. To the east of the broad antiformal structures, a tight syncline which is overturned to the east, is present. Its axial trace follows the valley between Mora and North Carmen. Evidence of an earlier deformation is present as mesoscopic folds of varying styles, with amplitudes ranging from several inches to a few feet. See figure 14. Mesoscopic folding is present in all units, but is most evident in the gneiss.

In order to delineate structural domain boundaries, a structure contour map was constructed using measured strike and dip values on the foliation. Due to the absence of a recognizable horizon within the gneiss, a phantom horizon was drawn at an initial elevation of 7000 feet. Measured attitudes of foliation were used to determine the position of all other contour lines on this surface.

The structural domains were labeled 1, 2, and 3, and are shown in plate 2. Subsequently, it was found necessary to subdivide domains 1 and 2, into 1a and 1b, and 2a and 2b, respectively. The structure contour map was also used to define the direction of plunge of the second deformation fold axes, B2. These folds are broad and asymmetrical, with vertical to overturned eastern limbs and moderately dipping western limbs.

A computer program, loaned by Professor A. J. Budding, was used to calculate the statistically best great circle fit to the foliation poles for domain 3.

In domains 1 and 2, the presence of bifurcating B2 fold axes reduced the data to the extent that only one limb of the B2 folds is defined clearly. For example, strike and dip readings in domain 1a define the western limb of a fold whose axis plunges in the direction N35W. The foliation data were insufficient to determine fold axes with the computer program. So the trends of the fold axes were determined visually from the structure map, for domains 1a, 1b, 2a, and 2b. A summary of the B2 trends in the different domains is included in Table 4.

On a stereonet, poles to cylindrically folded surfaces fall on a great circle, which is perpendicular to the axis, B [Dahlstrom, 1954]. Determination of this great circle is possible only if the data are well scattered, and include both limbs of the fold. However, in domains 1a, 1b, 2a, and 2b, the foliation poles plot as a maximum about one point. Unless the trend of the fold is known, a large number of great circles can be fitted to pass through this pole maximum, yielding a wide range of values for B. However, by using the visually determined trend for B, in

the respective subdomains, the corresponding plunge is easily calculated.

The trend and plunge of B, for domain 3, as determined with the computer program is in close agreement to that determined visually from the structure contour map and the equal area projection of figure 10.

More than 150 measurements of mesoscopic fold axes were made in the field. The data were plotted on a Schmidt equal area net with projection on the lower hemisphere for each of the three major structural domains. The diagrams were contoured as a percentage of points per one per cent area. The projections for domains 1, 2, and 3 are shown in figures 6 through 11.

Determination of B2 fold axes make possible the unrolling of the second deformation folds in order to get a prior orientation for the mesoscopic fold axes, B1. The B2 folds were unrolled to a point of horizontality, where the B1 axes are also horizontal. The resulting trends are summarized in Table 4.

Since we cannot assume that B1 fold axes were initially horizontal, an alternative and more correct method of determining the prior trend and plunge of the first deformation fold axes [Weiss and McIntyre, 1957], is to unroll the B2 folds such that the B1 axes describe small circles about the respective B2 axes. The intersection of all small circles, yields the prior trend and plunge of the B1 fold axes. See figure 12.

This method yields very interesting results. The point of small circle intersection, B_1 , for domains 1 and 2, about 57 degrees to S28W, is significantly different from the B1 maximum of domain 3. The structure contour map, plate 2, shows the reason for this discrepancy.

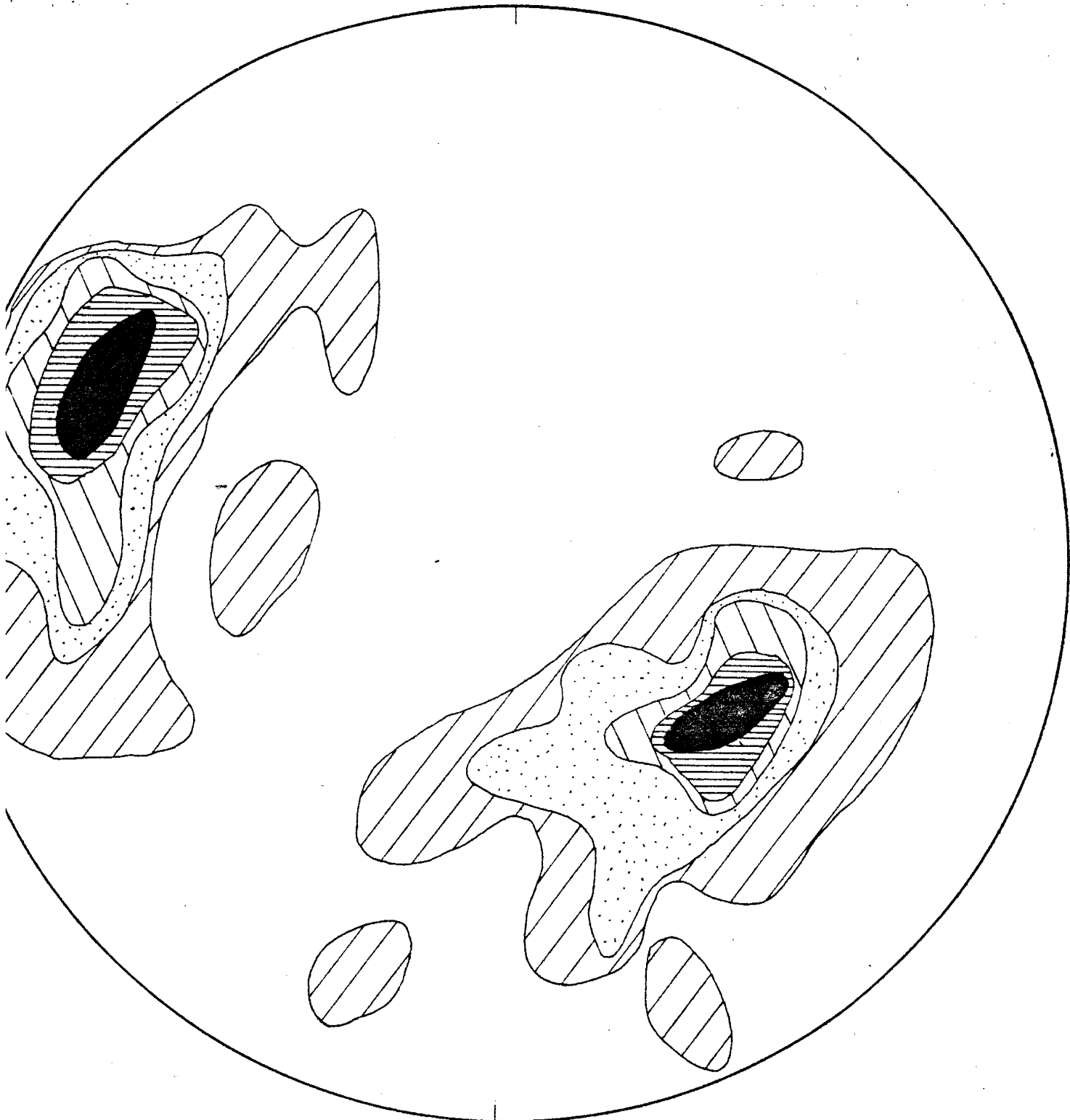
The general trend of B2 axes in domains 1 and 2 differs from that of

Figure 6.

Equal area projection of foliation poles in domain 1.

N

S



136 POLES TO FOLIATION

Domain I

LEGEND



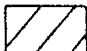

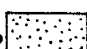

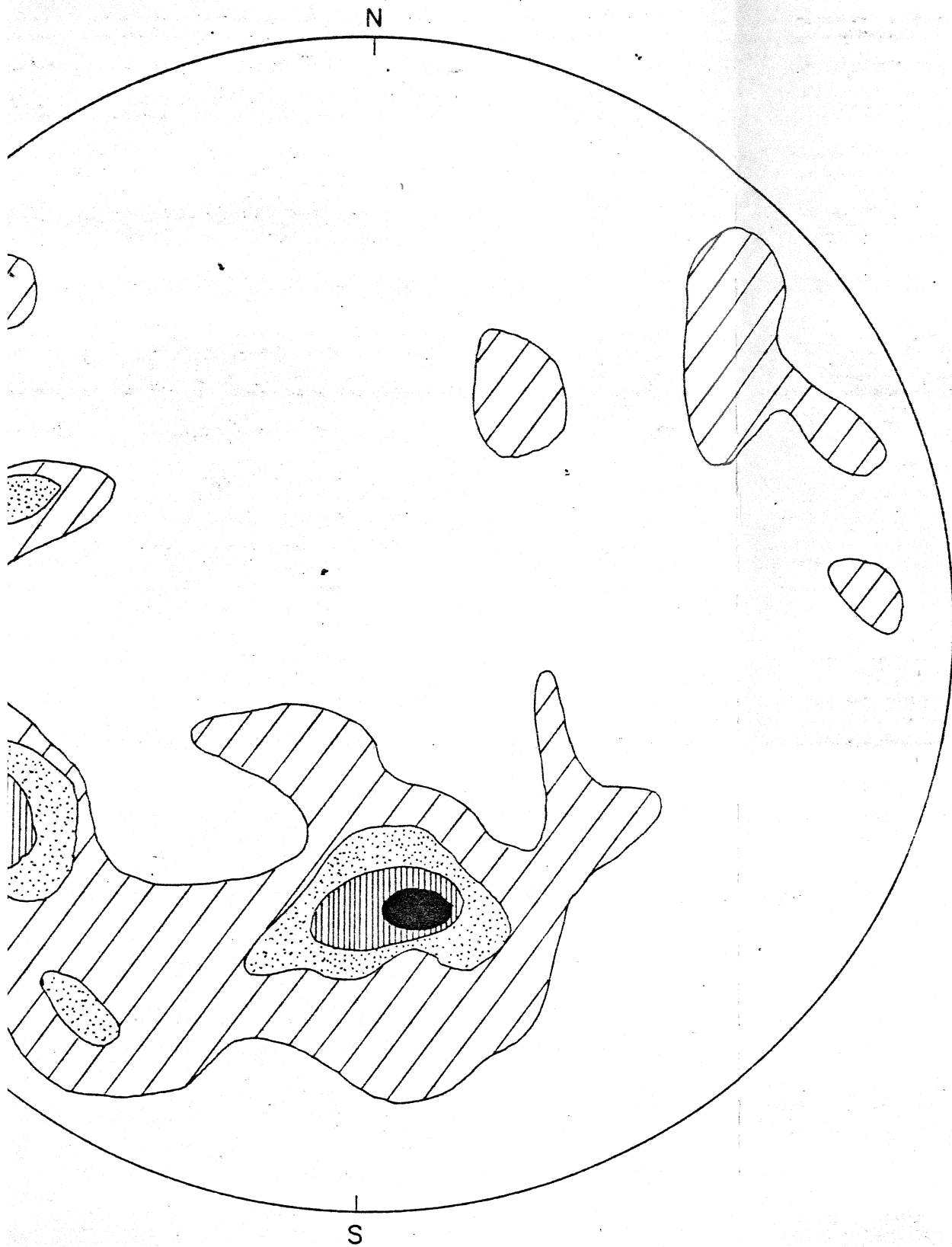
<0.7		4.4-6.6	
0.7-2.2%		6.6-8.8%	
2.2-4.4%		> 8.8%	

Figure 7.

Equal area projection of mesoscopic fold axes in domain 1.



LEGEND

65 FOLD AXIS

Domain I

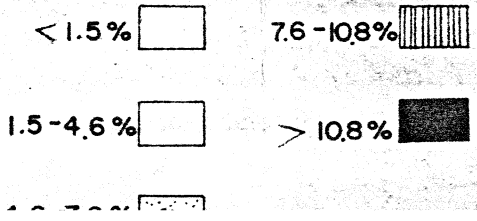
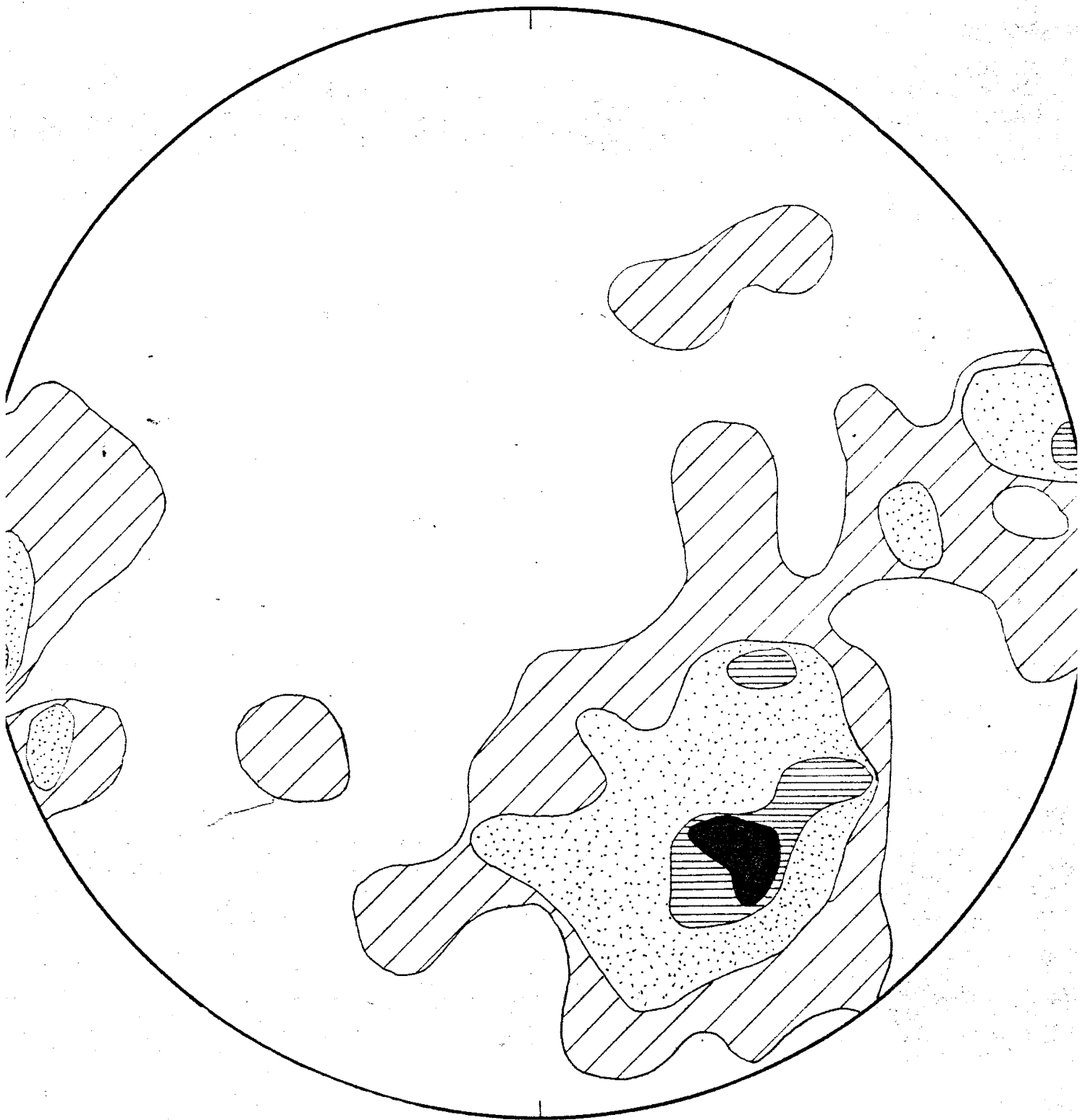


Figure 8.

Equal area projection of foliation poles in domain 2.

N





S


86 POLES TO FOLIATION

Domain 2

LEGEND

<1% 

6-9% 

1-3% 

> 9% 

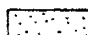
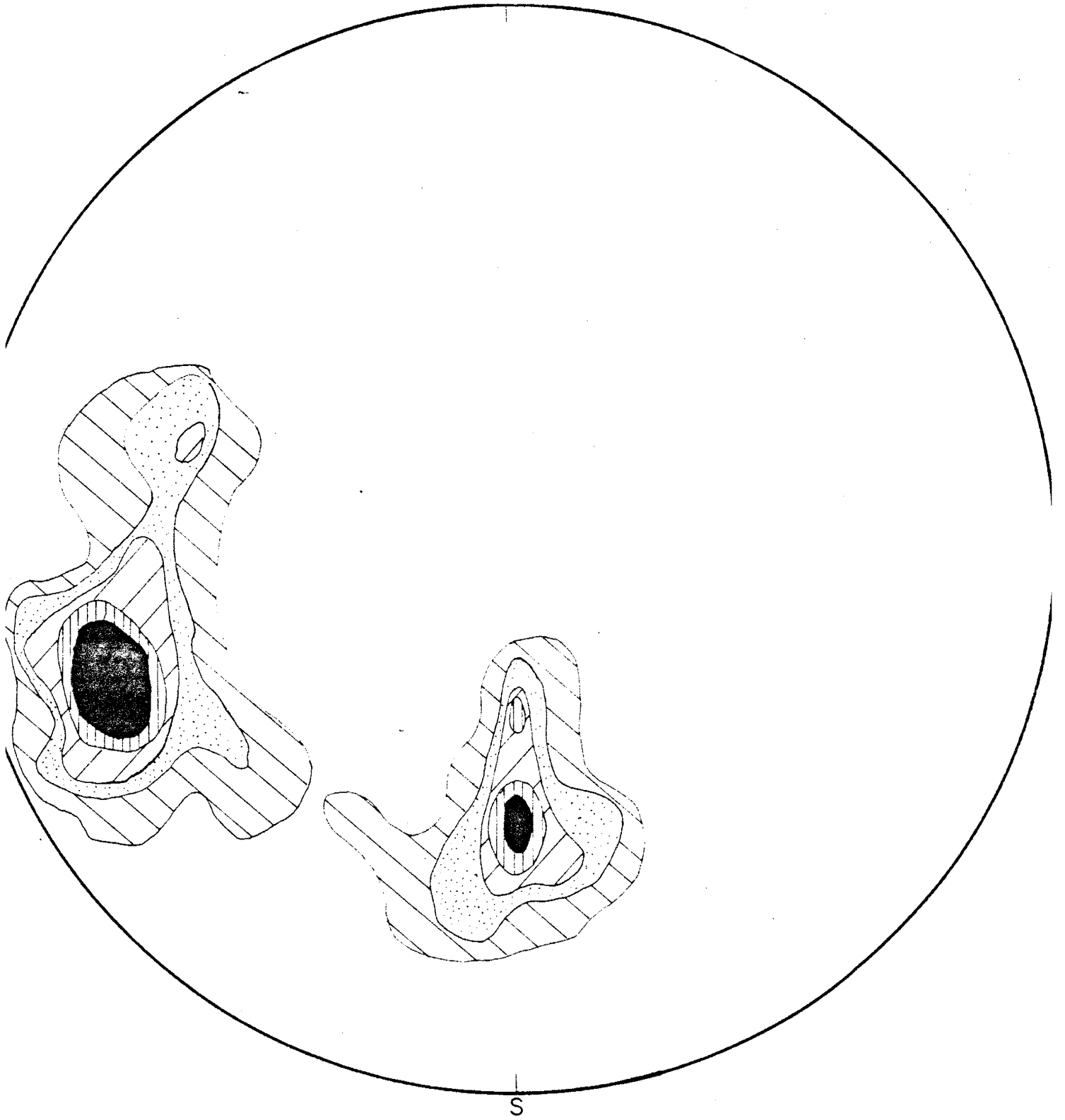
3-5% 

Figure 9.

Equal area projection of mesoscopic fold axes in domain 2.

N



S

64 FOLD AXIS

Domain 2

LEGEND

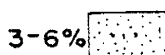
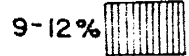
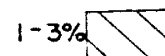
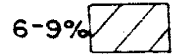
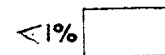
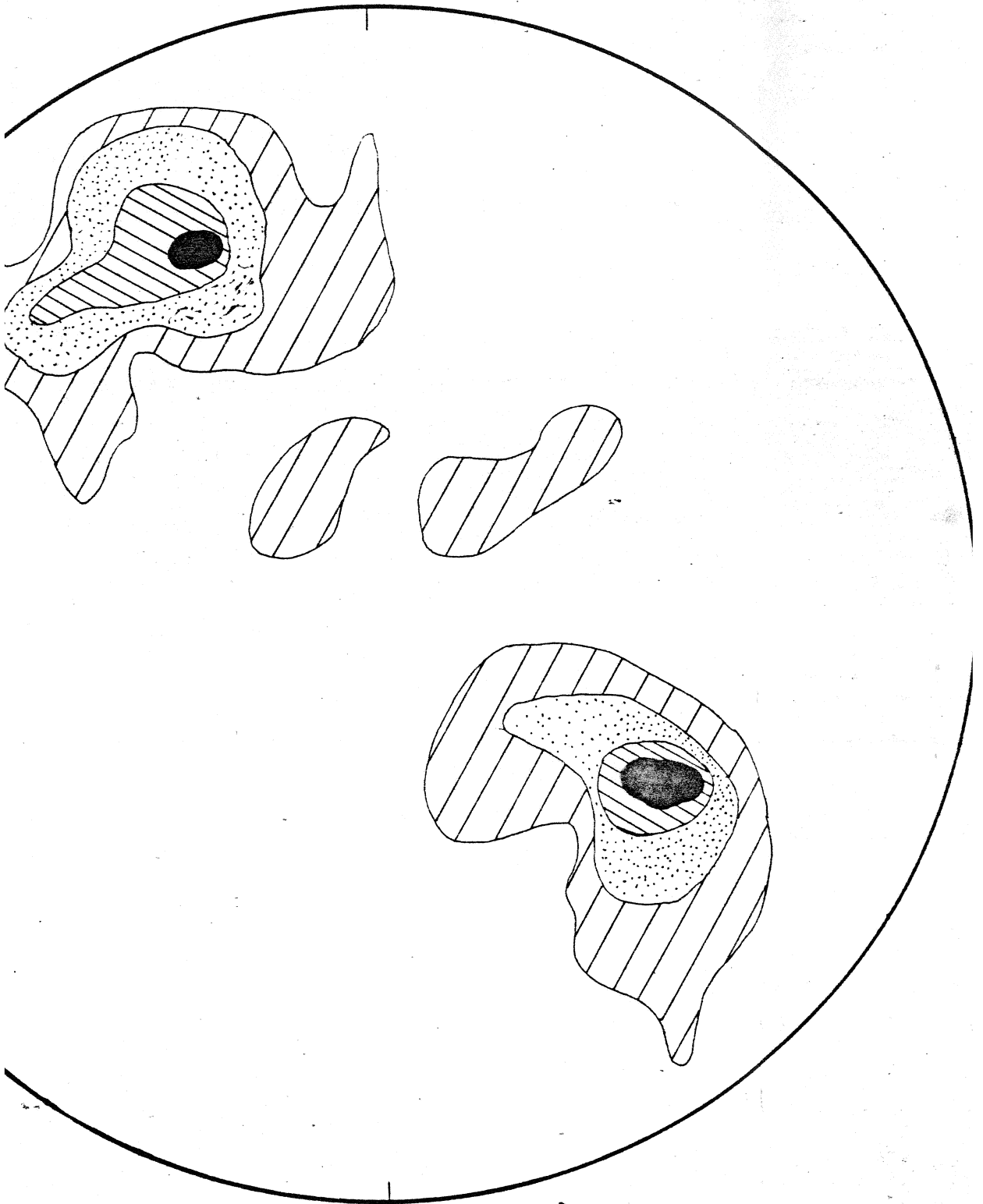


Figure 10

Equal area projection of foliation poles in domain 3.

N

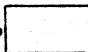


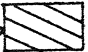
S


3 POLES TO FOLIATION

LEGEND

Domain 3

< 1.5% 

7.6-10.8% 

1.5-4.6% 


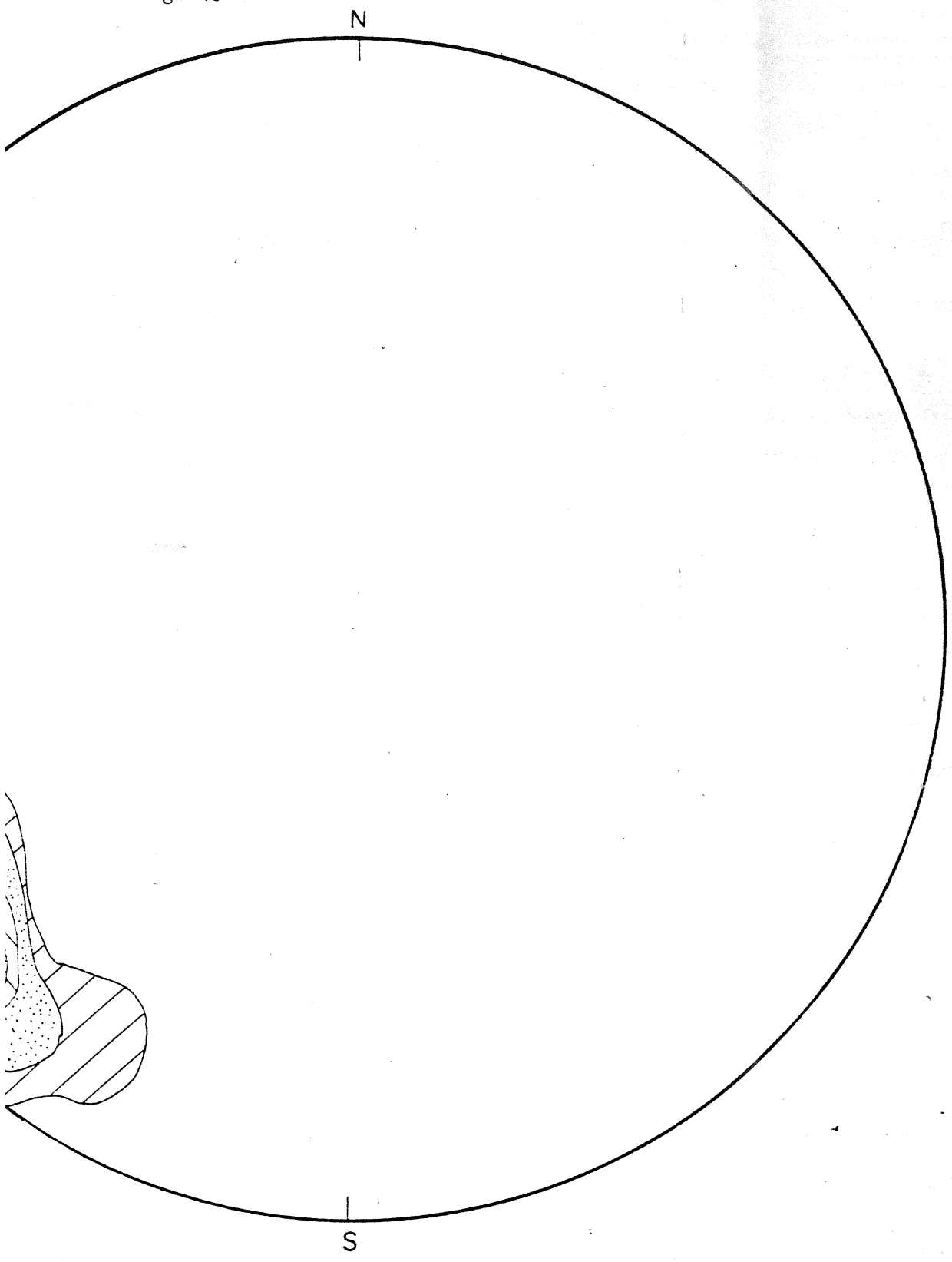
> 10.8% 

Figure 11.

Equal area projection of mesoscopic fold axes in domain 3.



FOLD AXIS

ain 3

LEGEND

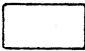

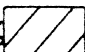
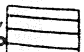
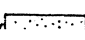

< 4%		16-24%	
4-8%		24-36%	
8-16%		36-60%	

Figure 12.

Diagram depicting method of determining prior orientation of
B1 axes, by intersecting small circles, in stereographic projection.

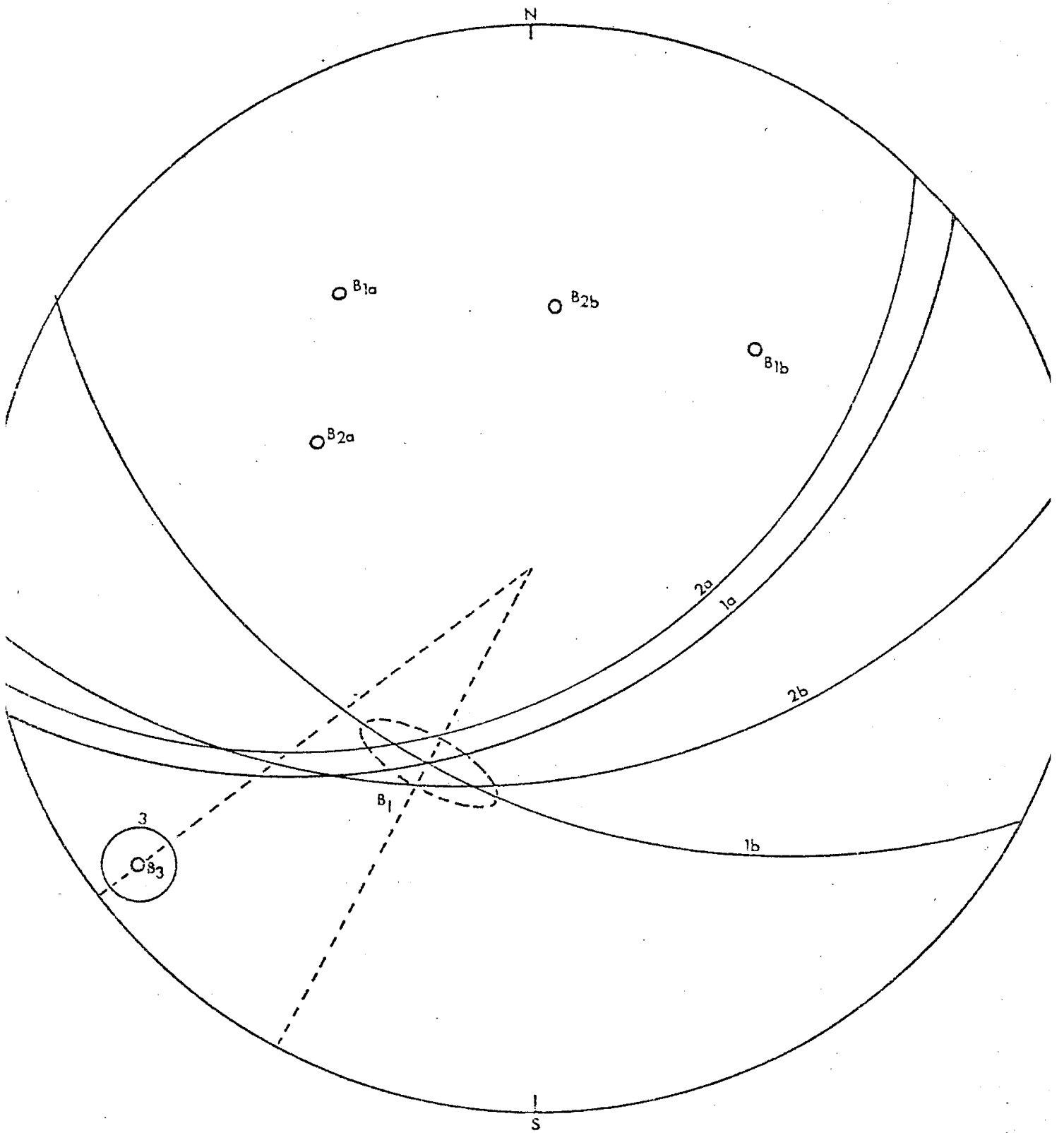


Table 4.

Summary of Structural Data Plotted in Stereographic Projection

Domain	Trend and Plunge of B	No. of Strike and dip readings	L1 Maxima	No. of Lineation readings	Trend of L1 axis after un- rolling to horiz.
1a	N35W, 38°	75	S64W, 24°	33	N70E
1b	N45E, 42°	61	S10E, 50°	32	N60E
2a	N60W, 52°	30	S72W, 24°	40	N60E
2b	N5E, 50°	56	S2E, 50°	24	N60E
3	S53W, 11°	63	S55W, 16°	26	N54E

domain 3 by about 25 to 30 degrees, the difference in trend between B3 and B_I. It appears from these data, that the B2 fold axes in domains 1 and 2 have been rotated in a northerly direction, by about 25 degrees, with respect to domain 3.

The difference in plunge is about 40 degrees. This difference is probably due to an upward rotation to the southwest, of domain 3. Such a movement would decrease the plunge of B1 and B2, in the southwest direction. This movement probably did not occur throughout the map area, as it would have the effect of increasing the plunge of B2 in the opposite direction, i.e. to the northeast, and, decreasing the southwesterly plunge of B1 axes in domains 1 and 2. However, B1 axes in these domains have a steeper southwesterly plunge than those in domain 3. These relationships can only be explained by a movement upward to the southwest, solely within domain 3. The prior orientation of B1 fold axes would thus be defined by B_I. The difference in trend and plunge between domain 3 and domains 1 and 2, could be the result of a third deformation, or a product of complex folding during the second deformation.

A survey of the literature, reveals structural trends similar to those in the El Oro Mountains, in the Precambrian of northern New Mexico.

Precambrian gneiss, immediately to the north of Mora, contains mesoscopic fold axes trending NNE [Riese, 1969].

Copper Mountain, in the Picuris Range, contains an anticlinal structure plunging 40 degrees to the ENE [Montgomery, 1953].

Precambrian rocks in the northern part of Taos County, are folded along N70E and N20W axes [McKinlay, 1957].

West of the Rio Grande, in La Madera Quadrangle, in Rio Arriba County,

planar structures striking N70W to S70W and dipping 60N to 60S, have been recorded [Bingler, 1965].

The northeasterly and southwesterly trends present in the El Oro Mountains have been well documented in the Precambrian of northern New Mexico. The mesoscopic folding which defined this trend is of varying styles. Two fold styles are shown in photographs in figure 13; sketches of other folds, from photographs and field notes, are shown in figure 14.

Similar folding was dominant during the first deformation. Isoclinal folding is well-developed throughout, but is most evident in the migmatitic gneiss, where quartzo-feldspathic banding delineates the folding. A few of the mesoscopic folds show evidence of superposed folding in outcrop, usually as harmonic undulations of the B1 fold limbs. Shearing, parallel to B1 axial planes has occurred, leaving the two fold limbs separated by a shear zone. These zones are often outlined by quartzo-feldspathic material. The axial planes of the B1 folds, in general, lie parallel to the foliation, indicating that the first folding was isoclinal.

Other linear structures include mineral and textural lineation and boudins.

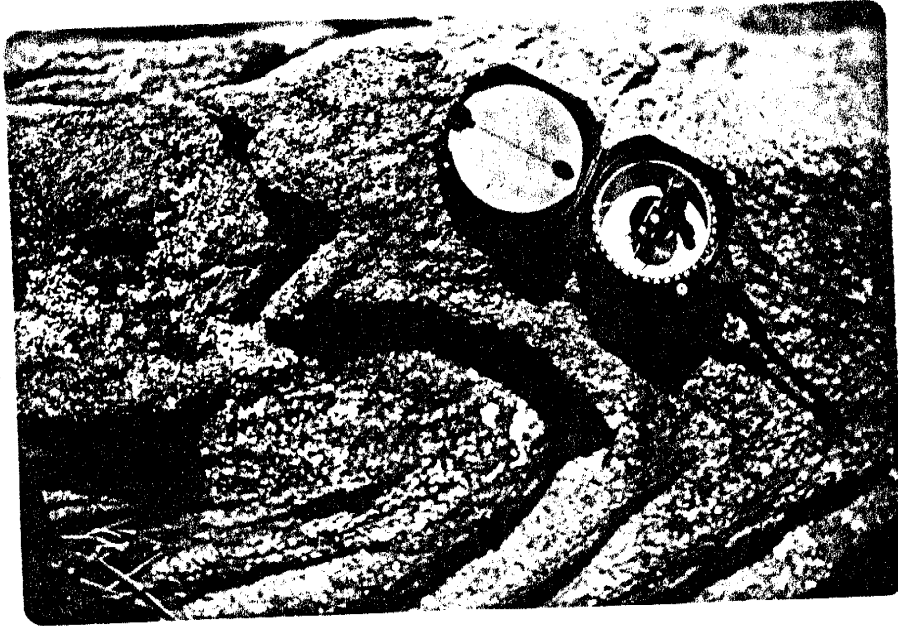
Mineral lineation, in the form of parallel prisms of hornblende within the amphibolite, have already been described. The prisms parallel the B1 axes in the area where they are found, although the evidence is meager.

Elongate feldspar and quartz aggregates are present in the gneiss west of Cebolla Pass. These rod-shaped aggregates are also parallel to B1 fold axes in that part of the map area.

Rotation of quartzite boudins has occurred within the amphibolite,

Figure 13.

- A Asymmetric similar fold in muscovite-rich gneiss,
south of Eagle Peak.
- B Chevron fold delineated by quartz-feldspar bands,
in the El Oro Mountains.



A

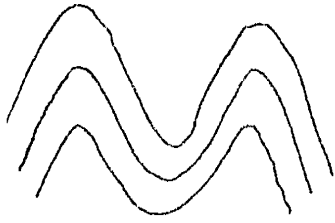


B

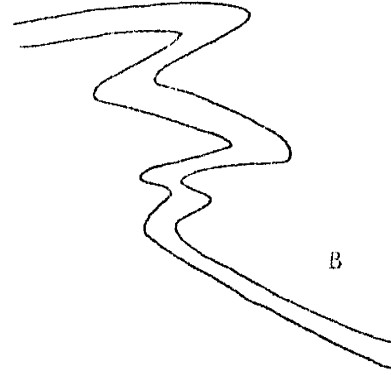
100-100
100-100

Figure 14.

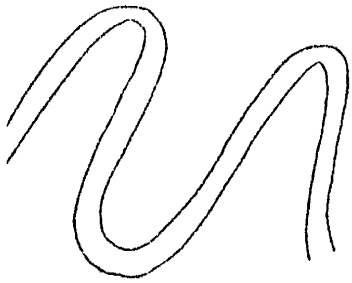
- A Symmetrical chevron fold in granitic gneiss, west of Eagle Peak.
- B Asymmetrical similar folding of quartz-feldspar band in biotite gneiss, southwest of Eagle Peak.
- C Open mesoscopic fold in muscovite gneiss.
- D Similar, asymmetrical folding of magnetite layers in gneiss, east of Eagle Peak.
- E Open similar mesoscopic fold showing evidence of superposed folding in harmonic undulations of limbs.
- F Similar folding with shear zone, parallel to axial plane of mesoscopic fold, delineated by quartzo-feldspathic material.
From a photograph taken west of Eagle Peak.



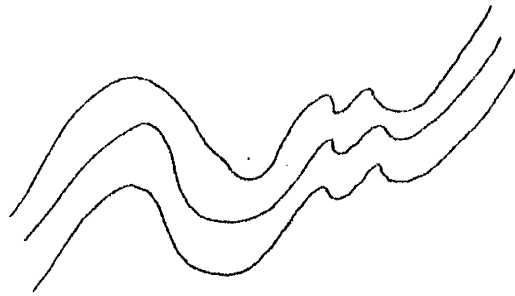
A



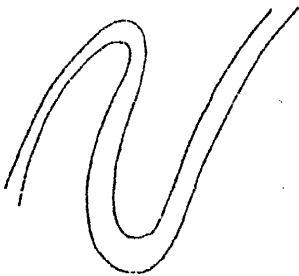
B



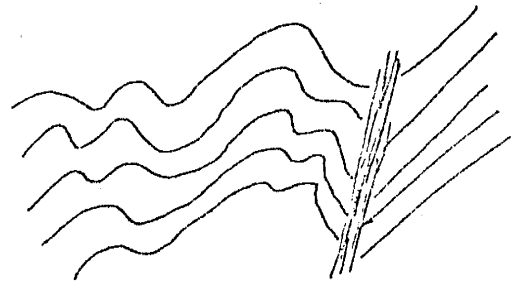
C



D



E



F

LIBRARY
UNIVERSITY OF TORONTO

west of Ledoux. The axis of rotation of the boudins plunges 10 degrees in the direction S40W. It is probable that rotation of these boudins occurred during the second deformation, which trends in the same direction in domain 3.

Faulting

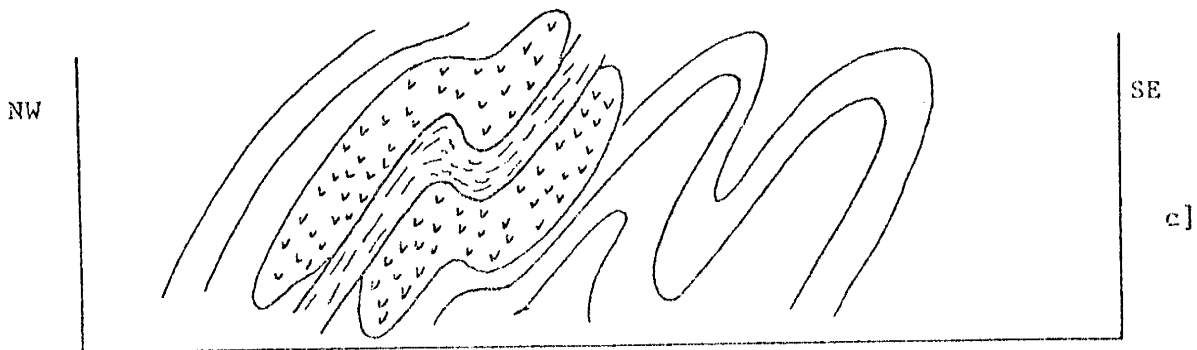
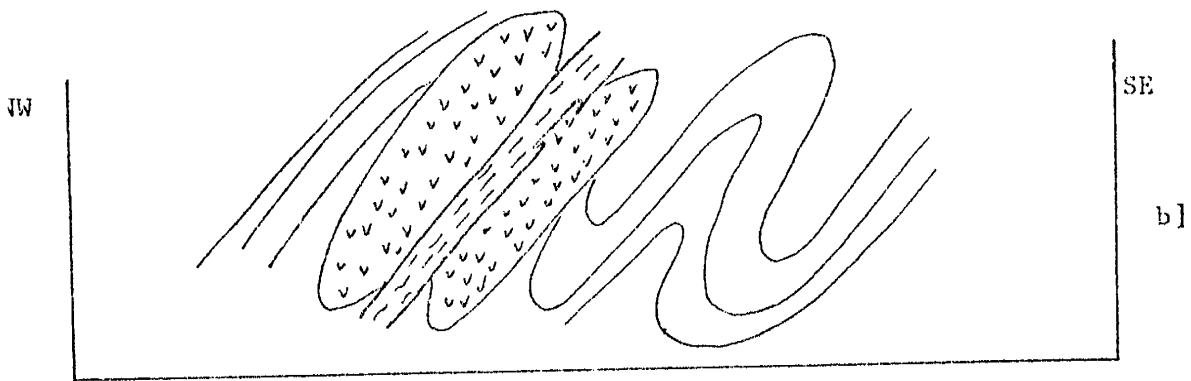
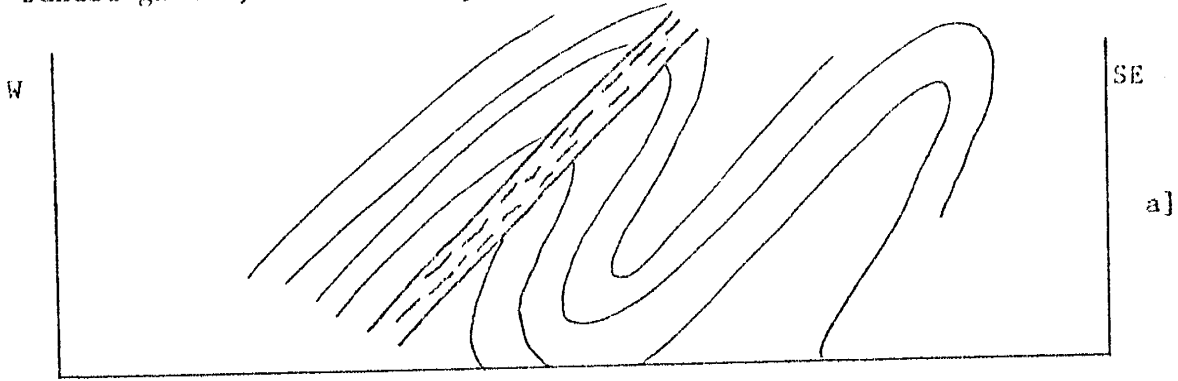
A Precambrian shear zone, preserved as banded gneiss, occurs northwest of Cebolla Pass. The orientation of this shear zone suggests that it was associated with isoclinal, recumbent folding overturned to the southeast. An idealized diagram of the formation of the shear zone, and accompanying intrusion of basic sills, is shown in figure 15. A later deformational phase has folded the banded gneiss into a small syncline, which is now exposed northwest of Cebolla Pass.

A more recent fault is exposed in the Precambrian northwest of Cebolla Pass. This fault strikes east-northeast and has faulted the older gneiss to the northwest against the younger amphibolite to the southeast. The fault plane dips about 50 degrees to the northwest. Its extension under alluvium on either side of its exposure in the Precambrian, makes it impossible to determine whether this fault is pre- or post-Paleozoic. However, reverse faulting toward the east occurred during the Laramide deformation [Baltz and Bachman, 1956]; this fault probably dates from that period of crustal movement.

Small faults of Precambrian age, with displacements of several inches are present throughout the gneiss. Fault planes are often delineated by quartzo-feldspathic banding, and the plane of movement generally lies at

Figure 15

Schematic diagram showing, a) origin of shear zone, b) intrusion of basic sills adjacent to shear zone, and c) folding of shear zone, or banded gneiss, into small syncline.

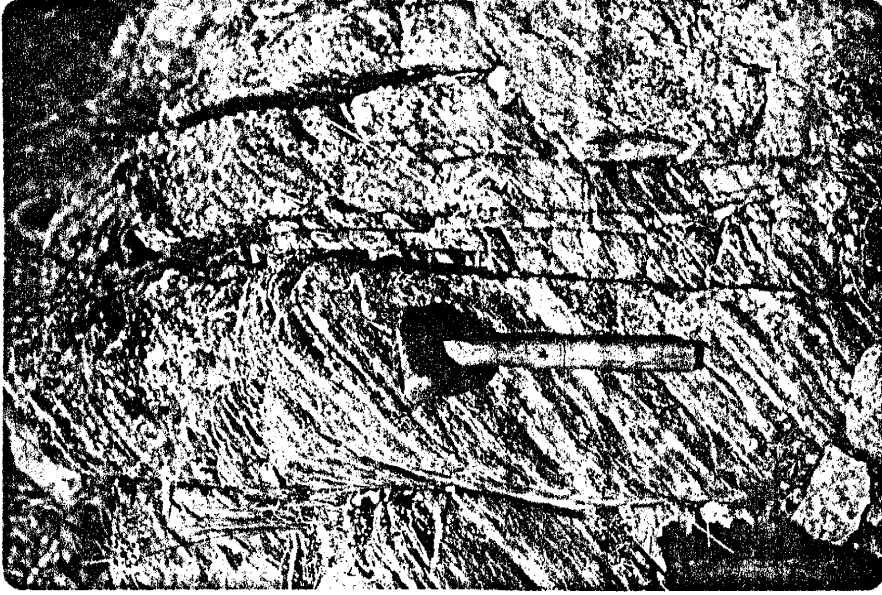


150-100
150-100

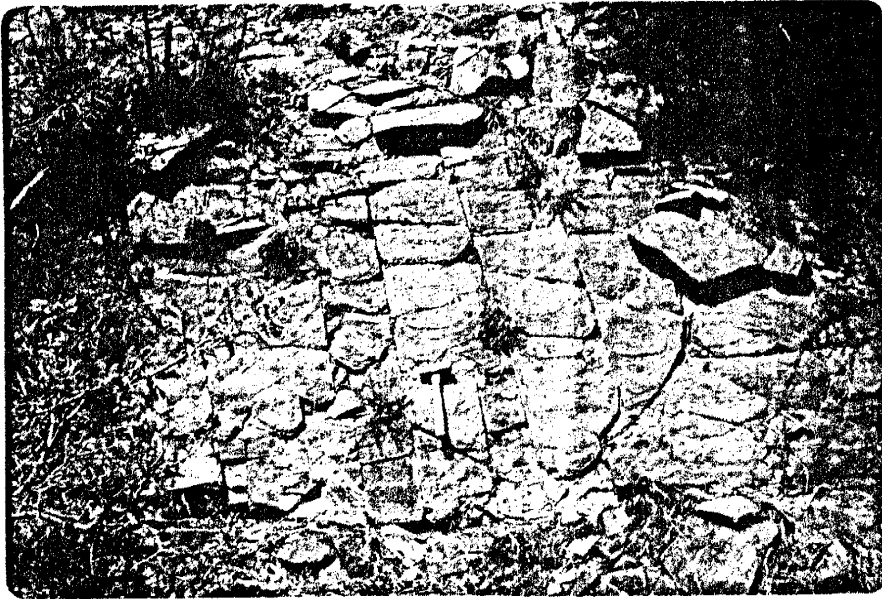
Figure 16.

A. Closely spaced parallel jointing east of Eagle Peak.

B. Jointing in massive amphibolite, in southwest part of map area.



A



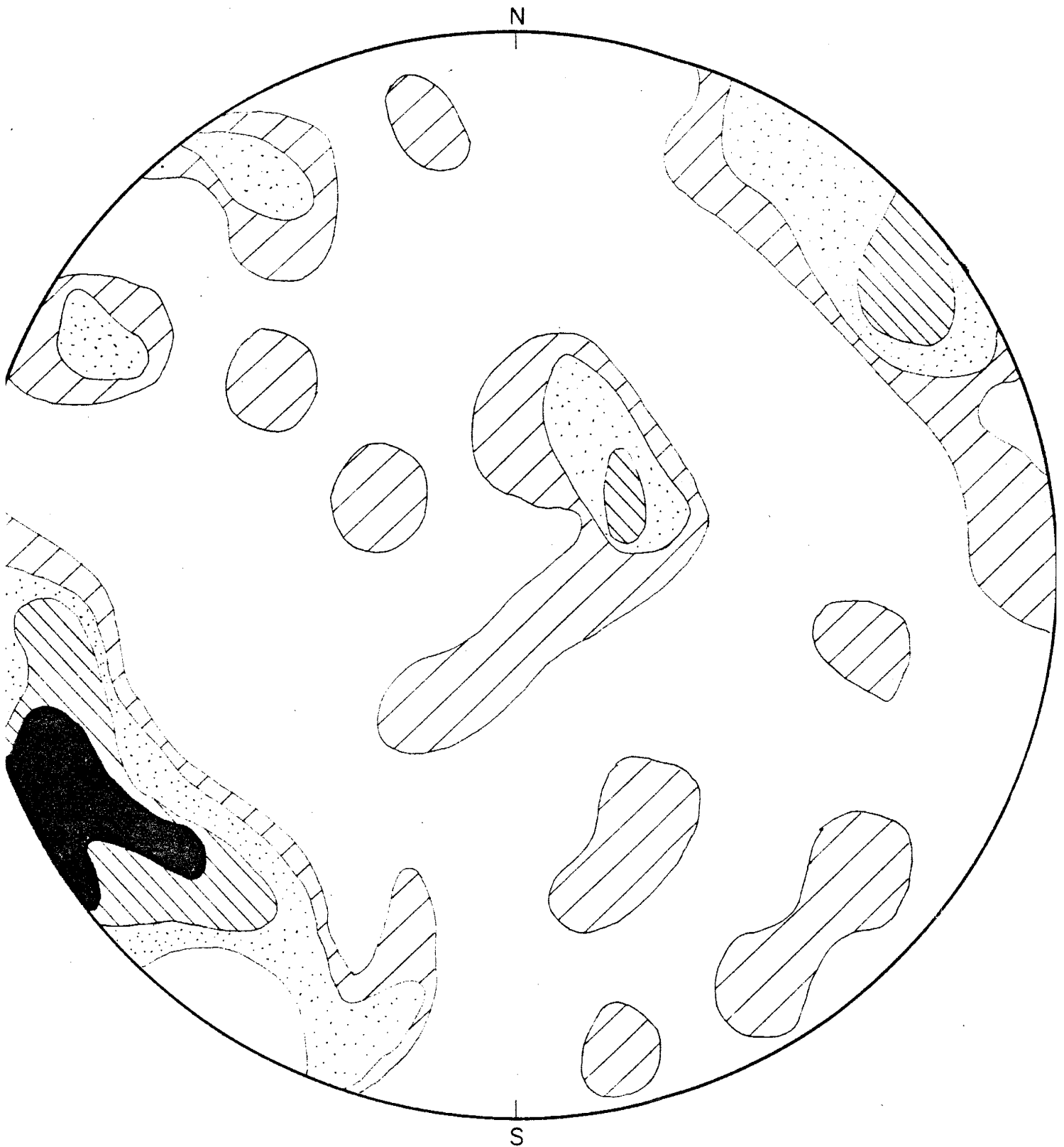
B

Figure 17.

Equal area projection of poles to joints in Precambrian rock units.


N

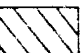
S

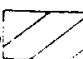


95 POLES TO JOINTS


LEGEND

< 1% 

4-6% 

1-2% 

> 6% 

2-4% 

a low angle to foliation.

Jointing

Two types of jointing were measured in the field. A large well-defined jointing forms large fracture surfaces, commonly in two directions at right angles to each other. The spacing ranges from a few feet to several hundred feet. Closely spaced, parallel joints, interpreted as fold cleavage, are also present. See figure 16.

The few measurements of fold cleavage, plotted on the stereographic net, did not deviate from the orientation of the large-scale jointing, therefore, all joints were plotted on the same equal area net [figure 17]. In general, the strike of the joints is perpendicular to the trend of the B_2 fold axes.

GEOLOGIC HISTORY

During Precambrian time, arkosic sandstones, perhaps derived from an older metamorphic or igneous complex, interbedded with locally iron-rich quartz arenites, and aluminous shales, were laid down as part of a sedimentary sequence.

Later, but still during the Precambrian, isoclinal, recumbent folding, overturned to the southeast occurred, as evidenced by mesoscopic folds within the gneiss and mantling units. The quartzo-feldspathic bands which outline these folds, indicate that this period of deformation was accompanied by metamorphic conditions intense enough to produce a migmatitic gneiss from the arkosic sandstones in the sequence. Iron-rich quartz arenites were transformed to magnetite-bearing quartzite beds, and aluminous shales were metamorphosed to muscovite schist.

A decrease in pressure and temperature, and the presence of a stress field with an orientation similar to that responsible for the earlier folding, produced an east-northeast trending shear zone in the northwest part of the map area. Adjacent to this zone of weakness, and in other parts of the sequence, gabbroic sills were intruded.

Subsequently, but still during Precambrian time, a second period of deformation, characterized by broad domal structures trending northeast-southwest, predominated, and is also responsible for the small syncline in which the banded gneiss occurs. This deformational phase was accompanied by metamorphic conditions as high as the amphibolite facies, as the gabbroic sills were metamorphosed to amphibolites. This later period of metamorphism obliterated the cataclastic texture of the

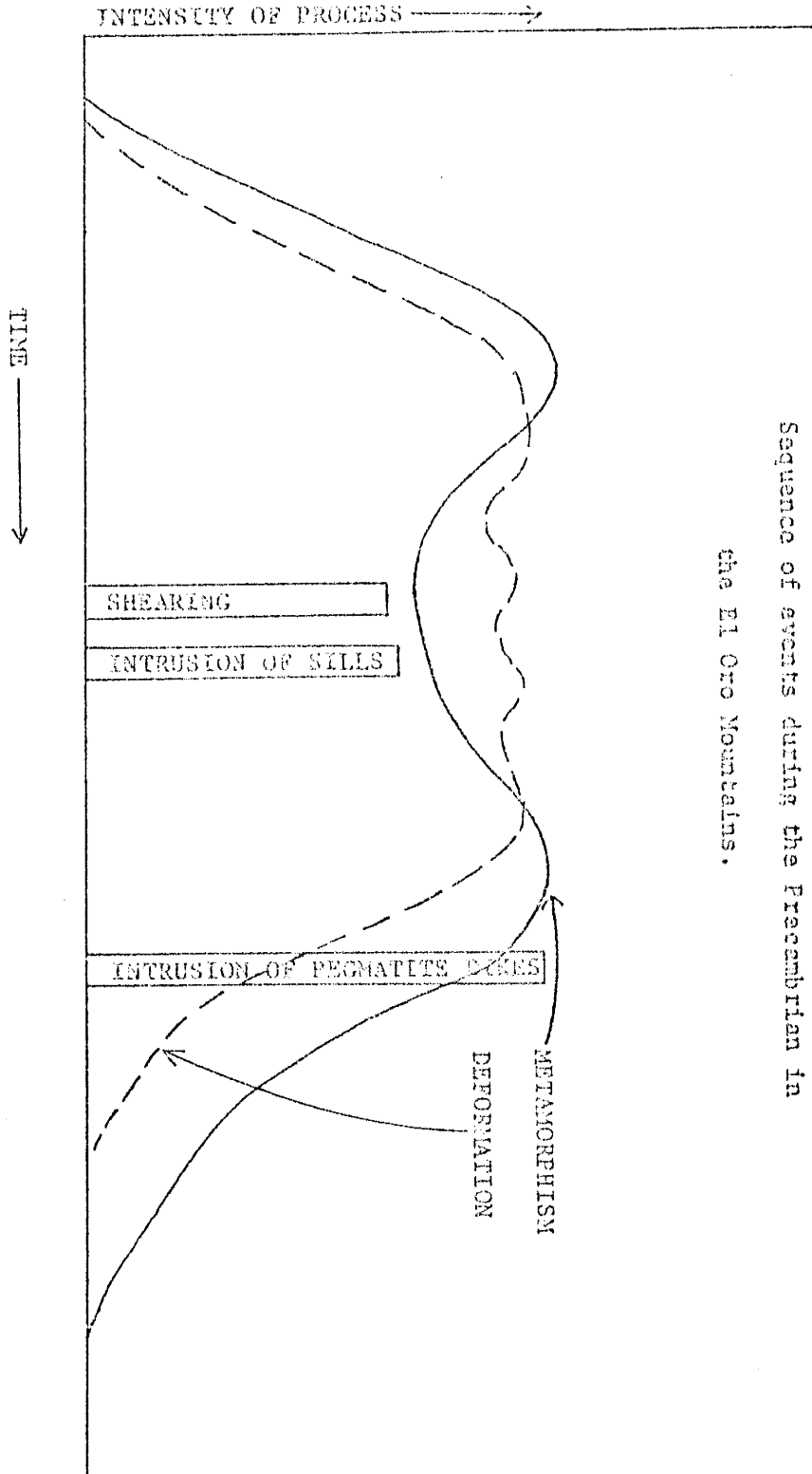


Figure 18.
Sequence of events during the Precambrian in
the El Oro Mountains.

shear zone and accentuated the mechanical differentiation produced by shearing. The banded gneiss is thus the result of processes of shearing and recrystallization.

In the waning stages of the latest Precambrian deformation and metamorphism, muscovite-rich pegmatite dikes intruded the sequence parallel to foliation. A schematic diagram of the sequence of events during Precambrian time is shown in figure 13.

A rubidium-strontium analysis [Graham, Shell publ. 429] of orthoclase from a core of the basement, from a well seven miles northeast of Guadalupe, indicates an age of approximately 1 billion years. Guadalupe is approximately 14 miles north of Mora. According to Graham, the core sample is similar to the biotite gneiss in the Mora area. This age substantiates the supposition that the metamorphism is Precambrian in age.

In late Precambrian and early Paleozoic time the area was eroded, and subsequently, a sequence of late Paleozoic limestones and sandstones was deposited on the Precambrian rocks.

During the Laramide deformation, reverse faulting to the east occurred. The fault exposed north of Cebolla Pass probably dates from this period of deformation.

Since that time, erosion has been dominant in this part of the Sangre de Cristo Mountains, stripping away the mantle of Paleozoic sediments to expose the Precambrian in the El Oro Mountains. A thin cover of alluvium was deposited in the valleys.

REFERENCES CITED

- Bailey, E.H., and Stevens, R.E., 1960, Selective staining of K-feldspar and plagioclase on rock slabs and thin-sections: *Am. Mineralogist*, v. 45, p. 1020-1025.
- Baltz, E. H., and Bachman, C.O., 1956, Notes on the geology of the southeastern Sangre de Cristo Mountains, New Mexico; *New Mexico Geol. Soc. Seventh Field Conf. Guidebook*, p. 96-108.
- Berthelsen, A., 1961, Structural classification of gneisses as used in teamwork in southwest Greenland: *Intl. Geol. Congress, Rept. of the 21st session*, p. 69-71.
- Bingler, E. C., 1965, Precambrian geology of La Madera Quadrangle, Rio Arriba County, New Mexico: *N. New. Inst. Min. and Tech., State Bur. Mines and Mineral Res., Bull. 80*, 132p.
- Binas, R. A., 1965, Hornblendes from some basic hornfelses in the New England region, New South Wales: *Min. Magazine*, v. 34, p. 52-65.
- Buddington, A.F., 1952, Chemical petrology of some metamorphosed gabbroic, syenitic, and quartz syenite rocks: *Amer. Jour. Sci., Bowen volume*, p. 37-84.
- Burnham, C.W., 1967, Hydrothermal fluids at the magmatic stage, in Barnes, H.L.[editor], *Geochemistry of Hydrothermal ore deposits*: New York, Holt, Rinehart, and Winston, Inc., p. 34-76.
- Cerny, P., 1971, Graphic intergrowths of feldspar and quartz in some Czechoslovak pegmatites: *Contr. Mineralogy and Petrol.*, v. 30, p. 343-355.
- Dahlstrom, C.D.D., 1954, Statistical analysis of cylindrical folds: *Can. Min. and Met. Bulletin*, v. 47, p. 234-239.

- Dierrich, R. V., 1960, Banded gneisses: Jour. of Petrology, v. 1, p. 92-136.
- , 1959, Banded gneisses of the Raudesund area, southeastern Norway: Norsk. Geol. Tidsskr., v. 40, pp. 13-63.
- Evans, B. W., 1965, Application of a reaction-rate method to the breakdown equilibria of muscovite and muscovite plus quartz: Amer. Jour. Sci., v. 263, p. 647-667.
- Engel, A. E. J., and Engel- C. G., 1962, Hornblendes formed during progressive metamorphism of amphibolites, northwest Adirondack Mountains, New York: Geol. Soc. America Bull., v. 73, p. 1499-1514.
- Graham, J. A., - - , Structural geology of the Mora area, Northeastern New Mexico: Shell Dev. Comp. Exploration and Production Res. Div., Publ. No. 429.
- Jahns, R. H., and Burnham, C. W., 1969, Experimental studies of pegmatite genesis: I. A model for the derivation and crystallization of granitic pegmatites: Econ. Geol., v. 64, p. 843-864.
- Luth, W. C., Jahns, R. H., and Tuttle, O. F., 1964, The granite system at pressures of 4 to 10 kilobars: Jour. Geophys. Res., v. 69, p. 759-773.
- Montgomery, A., 1953, Precambrian geology of the Picuris Range, north-central New Mexico: New Mex. Inst. Min. and Tech., State Bur. Mines and Mineral Res., Bull. 30, 89 p.
- McKinalay, P. F., 1956, Geology of Costilla and Latir Peak Quadrangles, Taos County, New Mexico: New Mex. Inst. Min. and Tech., State Bur. Mines and Mineral Res., Bull., 42.

- Quensel, P., 1917, Zur Kenntnis der mylonitbildung, erlautert an material aus dem Kebnekaisagebiet: Geol. Inst. Univ. of Upsala, v. 15, p. 91-116.
- Richardson, S. W., Gilbert, M. C., and Bell, P. M., 1969, Experimental determination of kyanite-andalusite and andalusite-sillimanite equilibria; the aluminum silicate triple point: Am. Jour. Sci., v. 267, p. 259-272.
- Riese, R., 1969, Precambrian geology of the southern part of the Rincon Range, New Mexico: unpub. M. S. Thesis, New Mex. Inst. Min. and Tech. 103p.
- Rivalenti, G., and Sighinolfi, G. P., 1971, The influence of the local pressure gradient and of the metamorphic grade on the composition of pegmatites in metamorphic terrains: Contr. Miner. Petrol., v. 34, p. 80-83.
- Schmakin, B. M., 1971, The role of pressure in geochemical differentiation of granites and pegmatites; Geochimica Intl., v. 3, p. 88-102.
- Segnit, R. E., and Kennedy, G. C., 1961, Relations in the system muscovite-quartz at high pressures: Am. Journal of Science, v. 259, p. 280-37.
- Shido, F., and Miyashiro, A., 1959, Hornblendes of basic metamorphic rocks: Jour. Sci. Fac. Univ. of Tokyo, v. 22, p. 88-102.
- Stanley, T., 1963, The Mora, New Mexico Story: Pep, Texas, 20 p.
- Weiss, L. E., and McLartyre, D. B., 1957, Structural geometry of Dalradian rocks at Loch Leven, Scottish Highlands: Jour. Geology, v. 65, p. 575-602.
- Winkler, H. G. F., 1967, Petrogenesis of metamorphic rocks: Springer Verlag Inc., New York, 237 p.

This thesis is accepted on behalf of the faculty of the
Institute by the following committee:

W. J. Prud'homme

Gale H. Bellings

Kent T. Cavalli

Date December 6, 1972